

# ERROR CONTROLLED REGULARIZATION BY PROJECTION\*

WOLFGANG DAHMEN<sup>†</sup> AND MARKUS JÜRGENS<sup>†</sup>

*Dedicated to Edward B. Saff on the occasion of his 60th birthday*

**Abstract.** The paper is concerned with regularization concepts for the inversion of diffusion processes. The application of the involved evolution operators is based on Dunford integral representations combined with the adaptive application of resolvents using recent wavelet methods. In particular, this allows us to develop and realize numerically, to our knowledge for the first time in this context, an SVD projection method which is compared to several versions of Tikhonov-type schemes. The theoretical findings are complemented by numerical tests shedding some light on the quantitative performance of the schemes.

**AMS Subject Classification:** 47A52, 65J20, 65J22

**Key Words:** Inverse problems, Dunford integrals, quadrature, Tikhonov method, projection methods, truncated SVD expansion, adaptive wavelet methods

**1. Introduction.** The notion of “inverse problem” serves as an important conceptual link between experimental and theoretical sciences. For example, unknown system parameters appearing in a model suggested by theory need to be retrieved from typically indirect measurements. “Given an answer one has to look for the question” which perhaps best reflects the typical ill-posedness of inverse problems. An important class of such even “severely” ill-posed inverse problems arises in connection with evolution equations of the form

$$\dot{u} + Au = 0, \quad u(0) = u_0, \quad (1.1)$$

where  $u$  is a function in time taking values in some Hilbert space  $X$  and  $A$  is a positive definite operator on  $\mathcal{D}(A; X) \subset X$ . When  $A = -\Delta$ , the negative Laplacian,  $X = L_2(\Omega)$ , where  $\Omega \subseteq \mathbb{R}^d$  is an open domain, this is the classical heat equation describing heat diffusion. The “solution” operator  $S$  that assigns to any initial data  $u_0$  the solution  $u(t)$  at later time  $t > 0$  is given by the operator exponential  $S = e^{-tA}$  and is known to define an analytic semigroup. When  $A : \mathcal{D}(A; X) \rightarrow X$  has an unbounded spectrum  $S$  will be compact. A classical inverse problem consists in finding the initial data  $u_0$  from the solution  $S(u_0)(t) = e^{-tA}u_0$  at some fixed time  $t > 0$ . Thus one has to “undo diffusion” which is expected to be a delicate task.

A similar situation arises with the inhomogeneous problem

$$\dot{u} + Au = f, \quad u(0) = 0,$$

where the solution operator is given by

$$(Sf)(t) = \int_t^T e^{-(\tau-t)A} f(\tau) d\tau. \quad (1.2)$$

These are special instances of the following general situation. Let  $S : X \rightarrow Y$  be a linear and compact operator between two Hilbert spaces  $X$  and  $Y$ . We aim at

---

\*This research was supported in part by the EEC Human Potential Programme under contract HPRN-CT-2002-00286, “Breaking Complexity”, and the SFB 401, “Flow Modulation and Fluid-Structure Interaction at Airplane Wings”, funded by the German Research Foundation

<sup>†</sup>RWTH Aachen, Institut für Geometrie und Praktische Mathematik, Templergraben 55, D-52056 Aachen, Germany

solving

$$Sx = y \tag{1.3}$$

for some given  $y \in Y$ . This equation has no solution unless  $y \in \text{Range}(S)$ . Even if  $y \in \text{Range}(S)$ , the solution is in general neither unique nor continuously depending on  $y$ . A way to restore uniqueness is to impose some additional selection criterion. A theoretical tool to solve (1.3) in this sense is the *Moore-Penrose generalized inverse*  $S^\dagger : \mathcal{D}(S^\dagger) \subset Y \rightarrow X$ ,  $\mathcal{D}(S^\dagger) = \text{Range}(S) \oplus \text{Range}(S)^\perp$ , defined by

$$x^\dagger = S^\dagger y = \int_0^{\|S\|^2} \frac{1}{\lambda} dE_\lambda S^* y,$$

where  $\{E_\lambda\}_{\lambda \geq 0}$  denotes the spectral family of the self-adjoint, compact operator  $S^*S$ . The integral converges if and only if  $y$  belongs to  $\mathcal{D}(S^\dagger; Y)$ . Thus when  $\text{Range}(S)$  is not closed  $y \in Y$  may fail to belong to  $\mathcal{D}(S^\dagger; Y)$ . Equivalently,  $x^\dagger$  can be defined as the *least-squares solution* of (1.3) with minimal norm, i.e.

$$\|Sx^\dagger - y\|_Y = \inf_{z \in X} \|Sz - y\|_Y$$

and  $x^\dagger$  has minimal norm among all  $z \in X$  for which the infimum is attained.

Still the unboundedness of the (generalized) inverse prevents a continuous dependence of the solution on the data so that *regularization* is necessary. Of course, this subject has been treated in numerous studies documented in the literature. The two most common regularization strategies are Tikhonov type schemes and projection methods. The numerical implementation of Tikhonov schemes requires the repeated approximate application of the solution operator and its dual which is typically done with the aid of time stepping schemes like the method of lines for the solution of the forward problem. This is computationally rather demanding while the so called “qualification” (limiting the attainable order of accuracy in terms of a decreasing noise level, see [9]) is only  $\mu_0 = 1$ . Among the class of projection methods a prominent role is played by truncated *singular value expansions* (SVD-expansions) which yield in some sense “optimal” projection methods, see e.g. [9]. Unfortunately the required system of singular basis functions is usually not numerically accessible at affordable cost.

The objective of this paper is to develop and analyze certain new variants of both strategies, Tikhonov and projection methods, for the inversion of diffusion processes. Since the essential algorithmic ingredients for the treatment of operators of the form  $S = e^{-tA}$  can be carried over to those given by (1.2) (see [15]) we shall exemplify matters for  $S = e^{-tA}$ . In Tikhonov schemes the explicit regularization parameter affects the whole spectrum of the operator. Therefore one might expect improvements from penalizing only the small part of the spectrum which will lead to one of the variants. This will be facilitated through certain projections based on representations as contour integrals in the complex plane similar to analogous representations of the solution operator itself. A central issue in this paper is therefore the development and analysis of error controlled numerical schemes for the evaluation of such integral representations which will allow us to completely avoid costly time stepping schemes in either regularization method. Perhaps more importantly, this will allow us to realize, to our knowledge for the first time, an efficient SVD-projection method for the inversion of diffusion processes without ever having to determine the singular basis functions.

Our schemes are based on a suitable quadrature rule for the contour integrals combined with an error controlled application of the involved resolvents at the quadrature points. A computationally attractive feature is that the different resolvent calculations are completely independent which leads to a trivial but highly efficient parallelization of the schemes. In principle, the resolvent equations (which are well-posed) can be solved by any discretization that guarantees a given accuracy tolerance. Here we shall employ recent adaptive wavelet schemes for the following reasons: Due to the induced norm equivalences, the wavelet setting allows us to realize conveniently the relevant topologies arising in this context and to control errors in the right norms. For instance, involved applications of resolvents can be performed with optimal complexity in the sense of [2] within desired error tolerances. Consequently, the application of the *true* operator exponential (not of  $e^{-tA_h}$  for some given discretization  $A_h$  of  $A$  and its inherited inaccuracy) can be given with rigorous accuracy bounds. In this sense the approach allows us to disentangle regularization and discretization of  $A$  in favor of transparent and accurate error bounds. Finally, the complexity results for the adaptive schemes from [2] will be seen to offer a first rough assessment of the computational complexity of the SVD-projection regularization. In this context one encounters a number of interesting questions that remain open but indicate in our opinion a promising potential of this approach.

It should be mentioned that a direct approximate application of the operator exponential can be also based on the *hierarchical matrix* concept, see e.g. [11]. However, this is an entirely discrete approach approximating  $e^{-tA_h}$  for a given matrix approximation  $A_h$  of  $A$ . Some comments on the resulting conceptual distinctions can be found at the end of Section 2.

The layout of the paper is as follows. In Section 2 we collect some basics from regularization theory and formulate the principal strategies. Section 3 is devoted to the concept of separating the spectrum of closed linear operators which our projection method will be based upon. We identify a contour integral representation of the boundedly invertible projection of  $S$  onto the eigenspace of  $A$  corresponding to a bounded part of its spectrum. This will serve later as the regularized approximation to  $S$ . In Section 4 we develop the main algorithmic ingredients based on suitable wavelet representations of the involved operators and corresponding adaptive evaluation scheme for their application within any desired accuracy tolerance. This is based on a suitable quadrature rule for the contour integrals as well as on an adaptive solution scheme developed in [2] for operators with sparse wavelet representations. These tools will be used to formulate and analyze in Section 5 several regularization schemes including modified Tikhonov schemes as well as the above mentioned new projection method. The latter one will be seen to offer much better efficiency than the Tikhonov-type schemes. Finally, in Section 6 the theoretical findings are quantified and illustrated by numerical experiments.

**2. Regularization.** We begin with briefly recalling some facts from regularization theory that will guide the subsequent developments, see [9] for details and proofs of the quoted results.

One way to approximate  $S^\dagger$  by a bounded function is to replace  $1/\lambda$  by a family of functions  $g_\alpha(\lambda)$ ,  $\alpha > 0$ , which are bounded and tend to  $1/\lambda$  pointwise if  $\alpha$  approaches zero. Abbreviating  $\|S\| := \|S\|_{\mathcal{L}(X,Y)}$ , the regularized solution is then defined as

$$x_\alpha = g_\alpha(S^*S)S^*y = \int_0^{\|S\|^2} g_\alpha(\lambda) dE_\lambda S^*y, \quad (2.1)$$

where the integral converges for every  $y \in Y$  as  $g_\alpha(\lambda)$  is bounded on  $[0, \|S\|^2]$ . In particular, the operator  $g_\alpha(S^*S)S^* : Y \rightarrow X$  is continuous with

$$\|g_\alpha(S^*S)S^*\| \leq \sup\{\sqrt{\lambda} |g_\alpha(\lambda)| : \lambda \in [0, \|S\|^2]\}.$$

The residual can be explicitly calculated as

$$\begin{aligned} x^\dagger - x_\alpha &= x^\dagger - g_\alpha(S^*S)S^*y = (I - g_\alpha(S^*S)S^*S)x^\dagger \\ &= \int_0^{\|S\|^2} r_\alpha(\lambda) dE_\lambda x^\dagger \end{aligned}$$

with

$$r_\alpha(\lambda) = 1 - \lambda g_\alpha(\lambda). \quad (2.2)$$

The approximation properties of this method are stated in the following theorem.

**THEOREM 2.1.** ([9], Theorem 4.1) *Let  $g_\alpha(\lambda) : [0, \|S\|^2] \rightarrow \mathbb{R}$  fulfill the following assumptions for all  $\alpha > 0$ :  $g_\alpha$  is piecewise continuous, there exists a constant  $C_g > 0$  independent of  $\alpha$  such that*

$$|\lambda g_\alpha(\lambda)| \leq C_g \quad \text{and} \quad \lim_{\alpha \rightarrow 0} g_\alpha(\lambda) = \frac{1}{\lambda} \quad \forall \lambda \in (0, \|S\|^2]. \quad (2.3)$$

Then

$$\lim_{\alpha \rightarrow 0} g_\alpha(S^*S)S^*y = S^\dagger y, \quad \text{if } y \in \mathcal{D}(S^\dagger), \quad (2.4)$$

and

$$\lim_{\alpha \rightarrow 0} \|g_\alpha(S^*S)S^*y\|_X = \infty, \quad \text{if } y \notin \mathcal{D}(S^\dagger). \quad (2.5)$$

Concrete rates of convergence in (2.4) can only be expected when  $x^\dagger$  belongs to some compact subset of  $X$  usually described in terms of ‘‘regularity’’ properties. A typical assumption leading to convergence rates is that  $x^\dagger$  belongs to the range of some power of  $S^*S$ . Knowing such a convergence rate would be important for dealing with *noisy* data  $y^\delta$  which are usually encountered in realistic applications. In fact, suppose that the noise level is  $\delta > 0$ , i.e.

$$\|y - y^\delta\|_Y \leq \delta.$$

Accordingly, one obtains perturbed results

$$x_\alpha^\delta = g_\alpha(S^*S)S^*y^\delta.$$

If a rate for  $\|x^\dagger - x_\alpha^\delta\|_X$  was known, in view of

$$\|x^\dagger - x_\alpha^\delta\|_X \leq \|x^\dagger - x_\alpha\|_X + \|x_\alpha - x_\alpha^\delta\|_X,$$

it would be sufficient to bound the ‘propagated error’  $\|x_\alpha - x_\alpha^\delta\|_X$  in order to balance both terms and thereby obtain the right regularization.

THEOREM 2.2. ([9], Theorem 4.2) *Let the assumptions of Theorem 2.1 be fulfilled and set for  $\alpha > 0$*

$$G_\alpha = \sup \{ |g_\alpha(\lambda)| : \lambda \in [0, \|S\|^2] \}.$$

*Then the estimates*

$$\|Sx_\alpha - Sx_\alpha^\delta\|_Y \leq C_g \delta, \quad \text{and} \quad \|x_\alpha - x_\alpha^\delta\|_X \leq \sqrt{C_g G_\alpha} \delta, \quad (2.6)$$

*hold true with  $C_g$  from (2.3).*

Thus, the propagated error stays proportional to the noise level  $\delta$  and a bound for  $\|x^\dagger - x_\alpha^\delta\|_X$  would tell us how to choose  $\alpha$ .

In practice, the necessary information is typically not available and a reasonable parameter value  $\alpha = \alpha(\delta, y^\delta) > 0$  has to be chosen for given data  $y^\delta$  in a different way. A widely used method is the *discrepancy principle* which defines

$$\alpha = \alpha(\delta, y^\delta) = \sup \{ \beta > 0 : \|Sx_\beta^\delta - y^\delta\| = \tau \delta \} \quad (2.7)$$

with some fixed parameter

$$\tau > \sup \{ |r_\alpha(\lambda)| : \alpha > 0, \lambda \in [0, \|S\|^2] \}.$$

Under fairly general conditions on  $g_\alpha(\lambda)$  convergence

$$x_{\alpha(\delta, y^\delta)}^\delta \rightarrow x^\dagger \quad \text{if } \delta \rightarrow 0,$$

of optimal order can be shown ([9], Theorem 4.17).

The strict condition (2.7) can be relaxed to finding the largest  $\alpha$  such that

$$\|Sx_\alpha^\delta - y^\delta\|_Y \leq \tau \delta \leq \|Sx_{2\alpha}^\delta - y^\delta\|_Y$$

holds which eases the use of the discrepancy principle.

Clearly,  $x_\alpha^\delta$  is generally again the solution of an operator equation. Thus, in practice, neither  $x_\alpha^\delta$  nor the residual  $\|Sx_\alpha^\delta - y^\delta\|_Y$  can be calculated exactly. Aiming at a rigorous error control we have to analyze the behavior of the discrepancy principle when both quantities are replaced by approximations  $\hat{x}_\alpha^\delta$  and  $\text{Res}_\alpha$ .

LEMMA 2.3. *Let  $\hat{x}_\alpha^\delta$  be a numerical approximation to the regularized solution  $x_\alpha^\delta$  satisfying*

$$\|\hat{x}_\alpha^\delta - x_\alpha^\delta\|_X \leq \tau_1 \|S\|^{-1} \delta. \quad (2.8)$$

*Moreover, suppose that the approximation to the true residual  $S\hat{x}_\alpha^\delta - y^\delta$  has norm  $\text{Res}_\alpha$  satisfying*

$$|\text{Res}_\alpha - \|S\hat{x}_\alpha^\delta - y^\delta\|_Y| \leq \tau_2 \delta, \quad (2.9)$$

*where the positive constants  $\tau_1, \tau_2$  are chosen such that*

$$\tau - \tau_1 - \tau_2 > \gamma := \sup \{ |r_\alpha(\lambda)| : \alpha > 0, \lambda \in [0, \|S\|^2] \}. \quad (2.10)$$

*Now let  $\alpha = \alpha(\delta, y^\delta)$  be chosen such that*

$$\text{Res}_\alpha \leq \tau \delta \leq \text{Res}_{2\alpha}. \quad (2.11)$$

Then the numerical approximations  $\widehat{x}_\alpha^\delta$  to the regularized solutions  $x_\alpha^\delta$  corresponding to the method  $(g_\alpha(S^*S)S^*, \alpha)$  converges in  $X$  to  $x^\dagger$  for  $\delta \rightarrow 0$  for all  $y \in \text{Range}(S)$ . In fact, it has optimal order  $\delta^{\frac{2\mu}{2\mu+1}}$  when  $x^\dagger \in \text{Range}(S^*S)^\mu$  for  $\mu \in (0, \mu_0 - 1/2]$ , where  $\mu_0$  is the “qualification” of the regularization method, see [9, Chapter 4.1].

*Proof.* We refer to the proof of Theorem 4.17 in [9] were the analogous statement is shown for the discrepancy principle with exact values of  $x_\alpha^\delta$  and  $\|Sx_\alpha^\delta - y^\delta\|_Y$ . A careful inspection reveals that the claim is reduced to verifying the two estimates

$$\|Sx_\alpha - y\|_Y \leq c_1\delta \quad \text{and} \quad \|Sx_{2\alpha} - y\|_Y > c_2\delta \quad (2.12)$$

for some constants  $c_1, c_2 > 0$ .

We infer the first part of (2.12) from the assumption  $\text{Res}_\alpha \leq \tau\delta$  as follows. One has

$$\begin{aligned} \|Sx_\alpha - y\|_Y &\leq \|Sx_\alpha^\delta - y^\delta\|_Y + \gamma\delta \leq \|S\widehat{x}_\alpha^\delta - y^\delta\|_Y + \|S\| \|x_\alpha^\delta - \widehat{x}_\alpha^\delta\|_X + \gamma\delta \\ &\leq \text{Res}_\alpha + \tau_2\delta + \tau_1\delta + \gamma\delta \leq (\tau + \tau_1 + \tau_2 + \gamma)\delta, \end{aligned}$$

where the first inequality results from the properties of  $r_\alpha(\lambda)$  and the definition of  $\gamma$ .

To see the second estimate of (2.12) we observe that

$$\begin{aligned} \|Sx_{2\alpha}^\delta - y^\delta\|_Y &\geq \|S\widehat{x}_{2\alpha}^\delta - y^\delta\|_Y - \|S\| \|x_{2\alpha}^\delta - \widehat{x}_{2\alpha}^\delta\|_X \leq \text{Res}_{2\alpha} - (\tau_1 + \tau_2)\delta \\ &> (\tau - \tau_1 - \tau_2)\delta. \end{aligned}$$

This implies  $\|Sx_{2\alpha} - y\|_Y \geq (\tau - \tau_1 - \tau_2 - \gamma)\delta$ , where  $\tau - \tau_1 - \tau_2 - \gamma$  is positive due to the choice of  $\tau$ ,  $\tau_1$ , and  $\tau_2$ .  $\square$

Loosely speaking, it is sufficient to keep the discretization errors proportional to the noise level. It should be noticed that this result is purely *asymptotic* for  $\delta \rightarrow 0^+$ . In particular, the constants  $\tau$ ,  $\tau_1$ , and  $\tau_2$  which heavily influence the outcome of numerical experiments can be chosen freely as long as (2.10) is satisfied.

It remains to specify the regularization method  $g_\alpha$ . Setting  $g_\alpha(\lambda) = (\alpha + \lambda)^{-1}$  yields the well-known *Tikhonov regularization* which reads

$$(\alpha I + S^*S)x_\alpha^\delta = S^*y^\delta. \quad (2.13)$$

$x_\alpha^\delta$  can equivalently be defined as solution of the minimization problem

$$\alpha \|x\|_X + \|Sx - y^\delta\|_Y \rightarrow \min_{x \in X},$$

which can be interpreted as compromise between the size of  $\|x\|_X$  and the residual error  $\|Sx - y^\delta\|_Y$ . It is well-known that in this case the qualification is  $\mu_0 = 1$ .

The penalization imposed by the Tikhonov scheme affects the whole spectrum of  $S^*S$ . This raises the question whether the resulting bias could perhaps be diminished by making the penalization dependent on the spectrum. In fact, it should be active only on the small eigenvalues of  $S^*S$ . Thus, a first alternative is

$$g_\alpha(\lambda) := (\alpha\chi_{[0,\alpha]}(\lambda) + \lambda)^{-1}. \quad (2.14)$$

This gives rise to what may be called “modified” Tikhonov regularization.

The second alternative deviates in a more essential way from the Tikhonov concept by taking

$$g_\alpha(\lambda) := \begin{cases} \frac{1}{\lambda}, & \lambda \geq \alpha; \\ 0, & \lambda < \alpha; \end{cases} \quad (2.15)$$

simply clipping the small eigenvalues of  $S^*S$ . This corresponds to setting the small singular values of  $S$  to zero and thus to a *truncated singular value expansion* which is known to be in some sense an “optimal” regularization method by projection. Moreover, in this case one has  $\mu_0 = \infty$ , see e.g. [9, Example 4.8]. We refer to this regularization scheme as SVD-projection. But of course, in practice the issue is to realize this projection method at affordable cost.

Both strategies (2.14), (2.15) hinge on the ability to realize *projections*  $Q_\alpha : X \rightarrow X$  taking  $X$  into an eigenspace corresponding to  $\sigma(S^*S) \cap [0, \alpha)$ . Then (2.14) gives rise to solving

$$(\alpha Q_\alpha + S^*S)x_\alpha^\delta = S^*y^\delta, \quad (2.16)$$

while (2.15) leads to

$$R_\alpha^* S^* S R_\alpha x_\alpha^\delta = R_\alpha^* S^* y^\delta, \quad R_\alpha := I - Q_\alpha. \quad (2.17)$$

We shall show below that for  $S = e^{-tA}$ ,  $A$  as in Section 1, such projections can be efficiently realized numerically which to our knowledge is new. Before addressing this in a systematic fashion, a few comments are in order. Of course, discretizations of  $A$  lead to approximations  $A_h$  of  $A$  defined on a finite dimensional subspace of  $X$  being now bounded with a norm depending on the discretization parameter  $h$ . Hence the spectrum of  $S_h = e^{-tA_h}$  is bounded away from zero so that solving

$$S_h^* S_h x_\alpha^\delta = S_h^* y^\delta \quad (2.18)$$

has a similar effect as (2.17) where e.g. the mesh size  $h$  of the underlying discretization acts as a regularization parameter. Solving (2.18) (which becomes increasingly ill-conditioned for  $h \rightarrow 0$ ) iteratively, the termination of the iteration adds another bias. Each application of  $S_h$  or  $S_h^*$  (either by approximately solving evolution equations or by employing  $H$ -matrix techniques, [11]) is inaccurate. For  $H$ -matrix concepts the problem is posed now in Euclidean metric which hampers somewhat taking the topological requirements of the original problem into proper account. So several sources of inaccuracies are mixed. We shall therefore pursue here a different line *separating* regularization and discretization. In particular, this will allow us to apply  $(R_\alpha^* S^* S R_\alpha)^{-1}$  for the “true”  $S$  within any desired tolerance. This will be based on two conceptual pillars: (a) the actual numerical realization of projections of the form  $Q_\alpha$  as well as of  $e^{-tA}$  within any desired target accuracy; (b) the involved application of resolvents  $(\gamma I - A)^{-1}$  appearing in the Dunford integral is based on adaptive wavelet schemes again realizing proper target accuracies without ever fixing any discretization of  $A$  beforehand.

We shall now fix our assumptions on the operator  $A$  which, of course, relates to the topologies of  $X$  and the image space  $Y$  under  $S$ .  $A$  will always be assumed to be *sectorial* and *normal* with spectrum in the right complex half plane. In particular, this covers selfadjoint positive definite operators. Moreover, it will be important to specify the mapping properties of  $A$ . To this end, we shall always assume to be given a Gelfand triple of Hilbert spaces  $H, V, H'$  satisfying

$$H \hookrightarrow V \hookrightarrow H', \quad (2.19)$$

where  $H'$  is the dual of  $H$  represented through the inner product  $\langle \cdot, \cdot \rangle := \langle \cdot, \cdot \rangle_{V \times V}$  of the pivot space  $V$ . In these terms we require that there exist bounded positive constants  $c_A, C_A$  such that

$$c_A \|v\|_H \leq \|Av\|_{H'} \leq C_A \|v\|_H, \quad u \in H. \quad (2.20)$$

i.e.  $A : H \rightarrow H'$  is a norm-isomorphism from  $H$  onto  $H'$ . A typical case is  $V = L_2(\Omega)$  and  $H = H_0^1(\Omega)$ ,  $H' = H^{-1}(\Omega)$  which fits to the heat equation with  $A = -\Delta$ , say. This will serve as a guiding example in the selfadjoint positive definite case.

In most part of the subsequent developments we shall have

$$V = X = Y, \quad (2.21)$$

which accounts for the fact that noise should not be measured in too strong a norm. Nevertheless, an alternative would be  $X = H'$ , so that  $\mathcal{D}(A; X) = H = Y$ , and later in Section 5.3 we shall encounter intermediate cases.

REMARK 1. *An analogous mapping property to (2.20) does not hold for  $S = e^{-tA}$ , i.e. we cannot find a pair of spaces for which an analogous estimate like (4.5) holds. Therefore, the concepts used e.g. in [3] do not apply in the present situation.*

**3. Separation of Spectrum.** We return to problems of the form (1.1). When  $X$  is a Hilbert space and  $A$  is self adjoint and positive definite there exists an orthonormal basis of eigenvectors  $\{x_k\}_{k \in \mathbb{N}}$  of  $A$  with associated eigenvalues  $\lambda_k > 0$ , sorted by decreasing size. Then, the operator exponential can be written as

$$e^{-tA}u_0 = \sum_{k=1}^{\infty} e^{-t\lambda_k} \langle u_0, x_k \rangle_{X \times X} x_k, \quad t \geq 0.$$

From this representation, it is immediately clear that

$$\|e^{-tA}u_0\|_X \leq e^{-t\lambda_1} \|u_0\|_X \quad \text{and} \quad \sigma(e^{-tA}) \setminus \{0\} = e^{-t\sigma(A)}, \quad t > 0.$$

Moreover, the eigenvector of  $e^{-tA}$  to the eigenvalue  $e^{-t\lambda_k}$  coincides with the eigenvector of  $A$  to the eigenvalue  $\lambda_k$ . This close relationship can be carried over to a more general situation as stated in the following theorem. To make that more precise, let us recall the following facts relating the spectrum of  $A$  to that of  $e^{-tA}$  even for the wider class of *sectorial operators*.

THEOREM 3.1. (Spectral mapping theorem, [10, 14]) *Let  $A$  be a sectorial operator on a Banach space  $X$ . For every  $t > 0$*

$$\sigma(e^{-tA}) \setminus \{0\} = e^{-t\sigma(A)} := \{e^{-t\lambda} : \lambda \in \sigma(A)\},$$

and

$$\sigma_p(e^{-tA}) = e^{-t\sigma_p(A)},$$

where  $\sigma_p$  denotes the point spectrum, i.e. the set of eigenvalues. Moreover, the eigenspaces of  $A$  and  $e^{-tA}$  are related by

$$\mathcal{N}(e^{-t\lambda}I - e^{-tA}) = \overline{\lim}_{k \in \mathbb{Z}} \mathcal{N}\left(\left(\lambda + \frac{2\pi ki}{t}\right)I - A\right)$$

for each  $t > 0$  and  $\lambda \in \mathbb{C}$ .

A representation of projections needed in (2.16), (2.17) can be based on the following principle, known as *separation of the spectrum*, that projects  $A$  as well as  $e^{-tA}$  onto the eigenvector spaces of  $A$  associated with a bounded subset of  $\sigma(A)$ .

To this end, assume that  $\sigma(A)$  is split into two disjoint, nonempty sets  $\sigma_1$  and  $\sigma_2$  such that  $\sigma_1$  lies in the interior of some Jordan curve  $\Gamma_1$  and  $\sigma_2$  in the exterior part. Then,

$$P := P_{\Gamma_1} := P_{\Gamma_1}(A) := \frac{1}{2\pi i} \int_{\Gamma_1} (\gamma I - A)^{-1} d\gamma \quad (3.1)$$



defines a bounded linear operator. Its basic properties can be summarized as follows.

**THEOREM 3.2.** (Theorem III.6.17 of [12]; Section 2.3 of [14])

*The operator  $P$  is a projection with  $\text{Range}(P) \subset \mathcal{D}(A^k; X)$  for every  $k \in \mathbb{N}$ . Moreover, setting*

$$Y_1 = P(X), \quad Y_2 = (I - P)(X),$$

$$A_1 : Y_1 \rightarrow Y_1 : x \mapsto Ax \quad \text{for all } x \in Y_1,$$

$$A_2 : \mathcal{D}(A_2) = \mathcal{D}(A; X) \cap Y_2 \rightarrow Y_2 : x \mapsto Ax \quad \text{for all } x \in \mathcal{D}(A_2),$$

*the operator  $A_1 : Y_1 \rightarrow Y_1$  is linear and bounded, and*

$$\sigma(A_1) = \sigma_1, \quad \sigma(A_2) = \sigma_2,$$

$$(\gamma I - A_1)^{-1} = (\gamma I - A)^{-1}|_{Y_1}, \quad \gamma \in \rho(A),$$

$$(\gamma I - A_2)^{-1} = (\gamma I - A)^{-1}|_{Y_2}, \quad \gamma \in \rho(A).$$

*If, in addition,  $X$  is a Hilbert space and  $A$  is normal, then  $P$  is the orthogonal projection onto  $Y_1$ .*

Thus,  $A$  is split into a bounded part  $A_1$  and an unbounded one  $A_2$ . As the projection  $P$  is defined by a curve integral similar to the definition of the operator exponential  $e^{-tA}$ , both are compatible in the following sense.

**PROPOSITION 3.3.** ([14], Prop. 2.3.3) *The projection  $P$  commutes with  $e^{-tA}$ , which implies  $e^{-tA}(Y_1) \subset Y_1$  and  $e^{-tA}(Y_2) \subset Y_2$ , i.e.  $Y_1$  and  $Y_2$  are invariant subspaces of  $X$  with respect to the semigroup.  $A_1$  and  $A_2$  generate semigroups in  $Y_1$  and  $Y_2$ , respectively, with*

$$e^{-tA_1} = e^{-tA}|_{Y_1} = e^{-tA}P|_{Y_1},$$

$$e^{-tA_2} = e^{-tA}|_{Y_2} = e^{-tA}(I - P)|_{Y_2}.$$

*As  $A_1$  is bounded,  $\{e^{-tA_1}\}_{t \geq 0}$  extends to a group  $\{e^{-tA_1}\}_{t \in \mathbb{R}}$ . In particular,  $e^{-tA_1}$ ,  $t > 0$ , is boundedly invertible with inverse*

$$(e^{-tA_1})^{-1} = e^{tA_1} = \frac{1}{2\pi i} \int_{\Gamma_1} e^{t\gamma} (\gamma I - A)^{-1} d\gamma.$$

*Moreover, for every  $\sigma > \sup\{\Re(\gamma) : \gamma \in \sigma_1\}$  there exists a constant  $M_\sigma \geq 1$  such that*

$$\|e^{tA_1}\|_X \leq M_\sigma e^{\sigma t}, \quad t \geq 0.$$

To see how this relates to an SVD-projection for  $S = e^{-tA}$ , suppose that the Jordan curve  $\Gamma_1$  encloses all (positive) eigenvalues of the operator  $B = A^* + A$  that are smaller than  $|\frac{1}{t} \log \frac{1}{\alpha}|$ . Recall that when  $A$  is normal the product  $S^*S$  takes the form

$$e^{-tA^*} e^{-tA} = e^{-tB}, \quad B = A + A^*, \quad (3.2)$$

a single exponential. Since by Theorem 3.1, any  $\xi \in \sigma(S^*S)$  has the form  $\xi = e^{-t\lambda}$ ,  $\lambda$  an eigenvalue of  $B$ , we infer from Proposition 3.3 and (2.17) that with the projection  $R_\alpha = P_{\Gamma_1} = P_{\Gamma_1}(B)$  with respect to  $B$  that

$$x_\alpha^\delta = (P_{\Gamma_1} S^* S P_{\Gamma_1})^\dagger S^* y^\delta = e^{tB_1} e^{-tA^*} y^\delta. \quad (3.3)$$

Hence the SVD-projection reduces here to the application of an exponential and a projected exponential.

Things simplify when  $A$  is selfadjoint and positive definite, so that singular values and eigenvalues coincide. Now one needs a curve enclosing all eigenvalues of  $A$  up to the size  $|\frac{1}{2t} \log \frac{1}{\alpha}|$  and a projection  $P_{\Gamma_1}(A)$  to obtain from (3.3), again in view of the properties stated in Proposition 3.3,

$$x_\alpha^\delta = e^{tA_1} y^\delta. \quad (3.4)$$

Thus regularization along this line amounts to just applying the inverse of a projected semigroup (and in the general case of an exponential) as opposed to solving operator equations of the type (2.13) or (2.16).

Of course, (3.4) can always be used in this form as long as the separation of spectrum is feasible, even when  $A$  is not selfadjoint. The regularization scheme (3.4) does then, however, not necessarily agree with an SVD-projection. For simplicity, we shall concentrate in what follows on (3.4), remarking that with the tools developed below, we could realize (3.3) as well.

We close this section with the following observation.

REMARK 2. *The projected semigroup provides also an efficient way for long time integration, i.e. to apply  $e^{-tA}$  for  $t \gg 0$ . Due to Proposition 3.3, one has*

$$\|e^{-tA}u_0 - e^{-tA}P_{\Gamma_1}u_0\|_X = \|(I - P)e^{-tA}u_0\|_X \leq e^{-t \inf \Re(\sigma_2)} \|u_0\|_X.$$

Thus, for  $\inf \Re(\sigma_2) > 0$  and  $t \rightarrow \infty$ , the semigroup  $e^{-tA}$  is closely approximated by the projected semigroup and it is sufficient to apply  $e^{-tA}P$  instead of  $e^{-tA}$ .

**4. Algorithmic Concepts.** For  $S = e^{-tA}$  the Tikhonov-type regularization strategies (2.13) and (2.16) require solving systems involving the products  $e^{-tA^*}e^{-tA}$ . Having iterative techniques in mind, this amounts to applying exponentials  $e^{-tA^*}$  and  $e^{-tA}$ . Moreover (2.16) and (3.4) involve applying projections of the above type  $P_{\Gamma_1}, I - P_{\Gamma_1}$ . The application of  $e^{-tA}$  has been thoroughly investigated e.g. in [11, 15, 16] taking again advantage of its representation of a Dunford integral now on a curve separating the whole spectrum of  $A$  from the rest of the complex plane. However, on account of Remark 2,  $e^{-tA}$  can be applied up to any desired accuracy also with the aid of a projected semigroup, so that we can confine the discussion here to the application of operators of the form

$$e^{-tA_1} = \frac{1}{2\pi i} \int_{\Gamma_1} e^{-t\gamma} (\gamma I - A)^{-1} d\gamma, \quad (4.1)$$

noting that the projection  $P_{\Gamma_1}$  is covered as a special case for  $t = 0$ . Hence, the common task is the application of the resolvents  $(\gamma_k I - A)^{-1}u_0 = v_{\gamma_k}$  and thus the solution of

$$(\gamma_k I - A)v_{\gamma_k} = u_0, \quad k = -N, -N + 1, \dots, N, \quad (4.2)$$

where  $\gamma_k = \gamma(kh)$  for  $k = -N, -N + 1, \dots, N$ , and fixed  $h > 0$  are quadrature nodes for a suitable parameterization of  $\Gamma_1$ .

In principle, every numerical scheme like FD, FEM or  $H$ -matrix techniques would be suitable, as long as assessable error bounds are available. Here our starting point is the following weak formulation of the resolvent equation  $(\gamma \text{id} - A)v = f$  where  $\gamma$

will always be assumed to belong to the resolvent set of  $A$ : for any given  $f \in H'$ , find  $u \in H$  such that

$$\langle A(\gamma)u, v \rangle = \langle \gamma^{-1}f, v \rangle \quad \text{for all } v \in H, \quad (4.3)$$

where

$$A(\gamma) := \text{id} - \gamma^{-1}A. \quad (4.4)$$

From (2.20) one can deduce that also

$$c_{A(\gamma)}\|v\|_H \leq \|A(\gamma)v\|_{H'} \leq C_{A(\gamma)}\|v\|_H, \quad u \in H. \quad (4.5)$$

holds for some constants  $c_{A(\gamma)}, C_{A(\gamma)} > 0$  that may depend on  $\gamma$ . Thus, for each  $\gamma$  (4.3) has a unique solution which depends continuously on the data  $f$ . However, we expect the ratios  $C_{A(\gamma)}/c_{A(\gamma)}$  to become large when  $\gamma$  gets close to the spectrum. Moreover, when  $|\gamma|$  grows  $A(\gamma)$  acts more and more like the identity on lower scales so that the mapping properties of  $A(\gamma)$  agree less and less with the topology of  $H$ .

This latter problem can be ameliorated by introducing appropriate  $\gamma$ -dependent norms on  $H$ . Such norms are conveniently realized by wavelet concepts. For the convenience of the reader, some basic ideas of wavelets for PDE's will be briefly sketched first. For an in depth discussion we refer to [2] and the references therein.

**4.1. Wavelets for Operator Equations.** We shall not give any details on specific realizations of wavelet bases but collect only their relevant properties. How to realize them has been discussed in the literature and we refer to references given e.g. in [7, 4]. As for some notational conventions, a wavelet basis will be denoted by  $\Psi = \{\psi_\lambda : \lambda \in \mathcal{J}\}$  where  $\mathcal{J}$  is a countable index set whose elements typically encode the scale, the spatial location and the type of the wavelets  $\psi_\lambda$ . The wavelets will always be assumed to be *local*, i.e.  $\text{diam}(\text{supp } \psi_\lambda) \sim 2^{-|\lambda|}$ , where  $|\lambda|$  denotes the scale, i.e. the dyadic refinement level on which the wavelet lives. Our first requirement is that  $\Psi$  be a *Riesz basis* for  $V$ . This means that every  $v \in V$  has a *unique* expansion  $v = \sum_{\lambda \in \mathcal{J}} \langle v, \tilde{\psi}_\lambda \rangle \psi_\lambda$  which is stable in the following sense. Denoting by  $\mathbf{v} = (v_\lambda)_{\lambda \in \mathcal{J}}$  the array of wavelet coefficients of  $v$ , there exists bounded constants  $c_R, C_R > 0$  such that

$$c_R\|\mathbf{v}\|_{\ell_2(\mathcal{J})} \leq \|v\|_V \leq C_R\|\mathbf{v}\|_{\ell_2(\mathcal{J})}, \quad v \in V. \quad (4.6)$$

It is well known that this implies the existence of a *dual* Riesz basis  $\tilde{\Psi} = \{\tilde{\psi}_\lambda : \lambda \in \mathcal{J}\} \subset V$  for  $V$ , i.e.  $\langle \tilde{\psi}_\lambda, \psi_{\lambda'} \rangle = \delta_{\lambda, \lambda'}$ , so that  $v_\lambda = \langle v, \psi_\lambda \rangle$ , and one has the alternate expansion  $v = \sum_{\lambda \in \mathcal{J}} \langle \psi_\lambda, v \rangle \tilde{\psi}_\lambda$ , see e.g. [5]. Viewing  $\Psi, \tilde{\Psi}$  as column vectors with respect to some fixed ordering of the indices,  $\langle v, \tilde{\Psi} \rangle, \langle \tilde{\Psi}, v \rangle$  are the arrays of wavelet coefficients in the first representation of  $v$  viewed as row and column vectors, respectively. The above expansions can then conveniently rewritten as

$$v = \langle v, \tilde{\Psi} \rangle \Psi = \langle v, \Psi \rangle \tilde{\Psi},$$

where we formally view the expansions as “inner products” of the coefficient arrays with the bases. As a default we shall view sequences as column vectors.

Moreover, a duality argument shows that in these terms

$$\frac{1}{C_R}\|\langle \tilde{\Psi}, v \rangle\|_{\ell_2(\mathcal{J})} \leq \|v\|_V \leq \frac{1}{c_R}\|\langle \Psi, v \rangle\|_{\ell_2(\mathcal{J})}, \quad v \in V.$$

For  $V = L_2(\Omega)$  and a wide range of domains one can construct  $\Psi$  and  $\tilde{\Psi}$  simultaneously in a way that the primal as well as dual wavelets are compactly supported. Moreover, these constructions actually offer more, namely that properly scaled versions of  $\Psi$  and  $\tilde{\Psi}$  form Riesz bases for certain smoothness spaces  $H, H'$ , respectively, appearing in (2.19). More precisely, for  $H$  from (2.19), we shall assume (in agreement with all known constructions) from now on that for the positive diagonal matrix

$$\mathbf{D} = \text{diag}\{d_\lambda : \lambda \in \mathcal{J}\}, \quad d_\lambda := \max\{1, \|\psi_\lambda\|_H\}, \quad (4.7)$$

one has

$$v \in H \iff \mathbf{D}\mathbf{v} \in \ell_2(\mathcal{J}), \quad \text{where } \mathbf{v} = \langle \tilde{\Psi}, v \rangle, \quad \text{i.e. } v = \mathbf{v}^T \tilde{\Psi},$$

and that the norm equivalence

$$c_H \|\mathbf{D}\mathbf{v}\|_{\ell_2(\mathcal{J})} \leq \|v\|_H \leq C_H \|\mathbf{D}\mathbf{v}\|_{\ell_2(\mathcal{J})}, \quad v = \mathbf{v}^T \tilde{\Psi} \in H, \quad (4.8)$$

holds with constants  $c_H, C_H > 0$ . Again it follows from biorthogonality and duality that

$$C_H^{-1} \|\mathbf{D}^{-1}\tilde{\mathbf{v}}\|_{\ell_2(\mathcal{J})} \leq \|v\|_{H'} \leq c_H^{-1} \|\mathbf{D}^{-1}\tilde{\mathbf{v}}\|_{\ell_2(\mathcal{J})}, \quad v = \tilde{\mathbf{v}}^T \tilde{\Psi} \in H'. \quad (4.9)$$

In these terms the rescaled bases  $\mathbf{D}^{-1}\Psi$  and  $\mathbf{D}\tilde{\Psi}$  are Riesz bases of  $H$  and  $H'$ , respectively.

This has been realized for Sobolev spaces  $H = H^t(\Omega)$  or  $H_0^t(\Omega)$ ,  $t < 3/2$ . In particular, for  $H = H_0^1(\Omega)$  the scaling weights are of the order  $d_\lambda = 2^{|\lambda|}$ . This suggests working with the rescaled bases exclusively, if one is only interested in the spaces  $H$  and  $H'$ . However, we are going to employ wavelet representations of operators from  $H$  onto  $H'$  (and even from  $H(\gamma) \rightarrow H(\gamma)'$  for certain  $V \subset H(\gamma) \subseteq H$ ) as well as of endomorphisms of  $V$ . Recording the dependence on  $\mathbf{D}$  (and further scalings) explicitly will enable us to adapt to the relevant topologies. Therefore, expansion coefficients will always relate to the  $V$ -normalized bases.

With these preparations we can transform now any variational problem of the form: Find  $u \in B$  such that for  $f \in H'$

$$\langle v, Bu \rangle = \langle v, f \rangle, \quad v \in H, \quad (4.10)$$

into an equivalent one in the wavelet coordinate domain. To this end, it will be convenient to define for any two countable collections  $\Theta, \Xi$  of functions, ordered in an unspecified but fixed way, the corresponding generalized Gramian by

$$\langle \Theta, \Xi \rangle := (\langle \theta, \xi \rangle)_{\theta \in \Theta, \xi \in \Xi},$$

i.e. the first entry is formally viewed as a column vector while the second one acts as a row vector which explains the subsequent formal manipulations. Using the scaled basis functions as test functions in (4.3), shows that the original variational problem (4.3) is equivalent to the infinite-dimensional system

$$\langle \mathbf{D}^{-1}\Psi, Bu \rangle = \langle \mathbf{D}^{-1}\Psi, f \rangle, \quad (4.11)$$

as  $\mathbf{D}^{-1}\Psi$  is complete in  $H$ . Inserting the representation  $u = \mathbf{u}^T \tilde{\Psi}$  into the previous equation, yields

$$\mathbf{D}^{-1} \underbrace{\langle \tilde{\Psi}, B\tilde{\Psi} \rangle}_{=\mathbf{B}} \mathbf{D}^{-1}(\mathbf{D}\mathbf{u}) = \mathbf{D}^{-1} \underbrace{\langle \tilde{\Psi}, f \rangle}_{=\mathbf{f}}. \quad (4.12)$$

$\mathbf{B} = \langle \Psi, B\Psi \rangle$  is called the (*standard*) *wavelet representation* of  $B$  with respect to  $\Psi$ . It is well known that, when  $B$  satisfies a relation like (2.20) and the basis satisfies (4.8), this latter problem is now well-posed in  $\ell_2(\mathcal{J})$ , see e.g. [2]. The relevant properties may be summarized as follows.

REMARK 3. *For every bounded linear operator  $B : H \rightarrow H'$  we have*

$$\|\mathbf{D}^{-1}\mathbf{B}\mathbf{D}^{-1}\|_{\mathcal{L}(\ell_2(\mathcal{J}),\ell_2(\mathcal{J}))} \leq C_H^2 \|B\|_{\mathcal{L}(H,H')}. \quad (4.13)$$

If (2.20) holds for  $B$  with constants  $c_B, C_B$ , i.e.  $B^{-1} \in \mathcal{L}(H',H)$  exists, we have

$$c_B c_H^2 \|\mathbf{v}\|_{\ell_2(\mathcal{J})} \leq \|\mathbf{D}^{-1}\mathbf{B}\mathbf{D}^{-1}\mathbf{v}\|_{\ell_2(\mathcal{J})} \leq C_B C_H^2 \|\mathbf{v}\|_{\ell_2(\mathcal{J})}, \quad \mathbf{v} \in \ell_2(\mathcal{J}). \quad (4.14)$$

i.e. the representation of  $B$  with respect to the scale basis  $\mathbf{D}^{-1}\Psi$  for  $H$ . Likewise, for every continuous endomorphism  $B : V \rightarrow V$  the estimates

$$\|\langle \Psi, B\Psi \rangle\|_{\mathcal{L}(\ell_2(\mathcal{J}),\ell_2(\mathcal{J}))} \leq C_R^2 \|B\|_{\mathcal{L}(V,V)} \quad (4.15)$$

and

$$\|\langle \tilde{\Psi}, B\tilde{\Psi} \rangle\|_{\mathcal{L}(\ell_2(\mathcal{J}),\ell_2(\mathcal{J}))} \leq c_R^{-2} \|B\|_{\mathcal{L}(V,V)} \quad (4.16)$$

are valid.

The property (4.14) provides one of the main foundations of the recent adaptive paradigm developed in [2]. In fact, it suggests that one can find simple preconditioners  $\mathbf{C}_n$  such that the idealized iteration

$$\mathbf{D}\mathbf{u}^{k+1} = \mathbf{D}\mathbf{u}^k + \mathbf{C}_n \mathbf{D}^{-1}(\mathbf{f} - \mathbf{B}\mathbf{u}^k), \quad k = 0, 1, \dots, \quad (4.17)$$

converges to the solution  $u = \mathbf{u}^T \Psi$  of (4.12) for any initial guess  $\mathbf{u}^0$  with some fixed error reduction rate  $\rho < 1$  per step. In fact, for symmetric positive definite  $B$  (implying that also  $\mathbf{B}$  is symmetric positive definite) the choice  $\mathbf{C}_n = \alpha \mathbf{I}$  would work for a suitable damping parameter depending on the constants in (4.14). In general,  $\mathbf{C}_n := \alpha(\mathbf{D}^{-1}\mathbf{B}\mathbf{D}^{-1})^T$  would in principle do the job although the corresponding squaring of condition numbers might degrade the quantitative performance.

For a numerical realization of (4.17), one has to approximate for any finitely supported input vector  $\mathbf{v}$  the infinite-dimensional vector  $\mathbf{D}^{-1}\mathbf{B}\mathbf{v}$  by some finitely supported  $\mathbf{w}$  that approximates the exact sequence  $\mathbf{D}^{-1}\mathbf{B}\mathbf{v}$  in  $\ell_2(\mathcal{J})$  within suitable dynamically updated tolerances. In fact, one actually applies compressed versions of  $\mathbf{D}^{-1}\mathbf{B}\mathbf{D}^{-1}$  to scaled vectors  $\mathbf{D}\mathbf{v}$ . These perturbations of the ideal iteration (4.17) can be shown to provide an adaptive solution scheme

$$\text{Solve}(\mathbf{D}, \mathbf{B}, \eta, \mathbf{f}) \rightarrow \mathbf{u}_\eta$$

that outputs for any target accuracy  $\eta > 0$  an approximate solution  $\mathbf{u}_\eta$  of  $\mathbf{B}\mathbf{u} = \mathbf{f}$  such that

$$\|\mathbf{D}(\mathbf{u} - \mathbf{u}_\eta)\|_{\ell_2(\mathcal{J})} \leq \eta, \quad (4.18)$$

which, in view of (4.8), means that  $\|u - u_\eta\|_H \leq C_H \eta$ .

Moreover, for operators  $B$  considered here one can contrive efficient schemes for the approximate application of  $\mathbf{D}^{-1}\mathbf{B}\mathbf{D}^{-1}$  so that the algorithm **Solve** can be shown to exhibit an overall asymptotically optimal work/accuracy balance in the following sense. To this end, let us denote for  $s > 0$  by  $\mathcal{A}^s = \mathcal{A}^s(H)$  the class of those

functions  $v \in H$  such that the error  $\sigma_N(v)$  of best  $N$ -term approximation of  $v$  in  $H$ , i.e., the accuracy obtainable by a linear combination of at most  $N$  wavelets, decays like  $N^{-s}$ . It is not hard to see that  $|v|_{\mathcal{A}^s} := \sup_{N \in \mathbb{N}} N^s \sigma_N(v)$  defines a quasinorm for  $\mathcal{A}^s$ . Moreover, when  $H = H^t(\Omega)$  for some  $t > 0$ , the space  $\mathcal{A}^s$  is almost characterized by the Besov space  $B_\tau^{t+s d}(L_\tau(\Omega))$ , where  $1/\tau = s + 1/2$ , see [2] for more details. Thus, an element  $v \in \mathcal{A}^s$  can be recovered within accuracy  $\eta$  using only the order of  $\eta^{-1/s} |v|_{\mathcal{A}^s}^{1/s}$  terms. It is important to note that, on account of (4.6), an element  $v = \mathbf{v}^T \Psi \in H$  belongs to  $\mathcal{A}^s$  if and only if its scaled wavelet coefficient array  $\mathbf{D}\mathbf{v}$  can also be approximated in  $\ell_2(\mathcal{J})$  within accuracy  $N^{-s}$  by the order of  $N$  terms. Equivalently, approximating  $\mathbf{v}$  in  $\ell_2(\mathcal{J})$  within a tolerance  $\eta > 0$ , takes the order of  $\eta^{-1/s} |v|_{\mathcal{A}^s}^{1/s}$  terms. Thus, in brief, (near-)best  $N$ -term approximation in  $H$  is directly linked to (near-)best  $N$ -term approximation in  $\ell_2(\mathcal{J})$ . Clearly, best  $N$ -term approximation in  $\ell_2(\mathcal{J})$  is conceptually very simple since it boils down to retaining the  $N$  largest terms in absolute value.

Now the main complexity estimate from [2] states that whenever the solution  $u$  of (4.10) belongs to  $\mathcal{A}^s$  for some  $s < s^*$ , then the computational work required by **Solve**( $\mathbf{D}, \mathbf{B}, \eta, \mathbf{f}$ ) to output an  $\eta$ -accurate approximation  $\mathbf{w}_\eta$  of  $\mathbf{u}$  and hence, in particular, the number of nonzero terms in  $\mathbf{w}_\eta$ , is bounded uniformly by  $\eta^{-1/s} |v|_{\mathcal{A}^s}^{1/s}$ . Moreover, when using spline wavelets of exactness order  $m \in \mathbb{N}$  it has been shown in [17] that the optimality range covers the highest possible order, i.e.  $s^* > m - t/d$ . For this optimal complexity estimate it is crucial to have a relation like (4.14) which requires controlling the constants in (4.8) and those in a mapping property like (2.20).

Now, in view of (4.2) or (4.3), we wish to apply **Solve** to the operators  $B = A(\gamma) = \text{id} - \gamma^{-1}A$  and denote the corresponding wavelet representations by  $\mathbf{A}(\gamma) = \langle \Psi, A(\gamma)\Psi \rangle$ . In principle, the above comments imply that, because of (4.5), the scheme **Solve** with the scaling  $\mathbf{D}$  would indeed work for each fixed  $\gamma$  in the resolvent set with optimal complexity. However, the number of iterations needed for a fixed error reduction depends on the ratio  $C_{A(\gamma)}/c_{A(\gamma)}$  so that the complexity bounds deteriorate with increasing  $C_{A(\gamma)}/c_{A(\gamma)}$ .

Of course, the lower constant will always depend on the *distance* of  $\gamma$  from the spectrum. To control this will be a matter of the choice of the curve  $\Gamma_1$ . So all one can hope for in addition is to reduce (or even avoid) the dependence of such stability constants on the *size*  $|\gamma|$ . To this end, we introduce next different norms on  $H$  and set

$$\mathbf{D}_\gamma = \text{diag}(d_\lambda(\gamma))_{\lambda \in \mathcal{J}}, \quad d_\lambda := \max\{1, |\gamma|^{-1/2} d_\lambda\}, \quad (4.19)$$

(with  $d_\lambda$  from (4.7)) and endow  $H$  with the norm

$$\|v\|_{H(\gamma)} := \|\mathbf{D}_\gamma \mathbf{v}\|_{\ell_2(\mathcal{J})}, \quad v = \mathbf{v}^T \Psi. \quad (4.20)$$

Clearly, by duality

$$\|w\|_{H(\gamma)'} = \|\mathbf{D}_\gamma^{-1} \langle \Psi, w \rangle\|_{\ell_2(\mathcal{J})}. \quad (4.21)$$

The analog to (4.8) holds for  $H(\gamma)$  trivially with constants  $c_{H(\gamma)} = C_{H(\gamma)} = 1$ . If we had in addition a mapping property

$$\hat{c} \|v\|_{H(\gamma)} \leq \|A(\gamma)v\|_{H(\gamma)'} \leq \hat{C} \|v\|_{H(\gamma)}, \quad v \in H(\gamma), \quad (4.22)$$

with constants independent of  $|\gamma|$ , we could conclude according to Remark 3 that

$$\text{kond}_2(\mathbf{D}_\gamma^{-1} \mathbf{A}(\gamma) \mathbf{D}_\gamma^{-1}) \sim 1, \quad (4.23)$$

which is needed for **Solve** to perform with asymptotically optimal complexity. To this end, it is easy to see that for  $v = \mathbf{v}^T \Psi$

$$\|A(\gamma)v\|_{H(\gamma)'} = \|\mathbf{D}_\gamma^{-1} \langle \Psi, A(\gamma)v \rangle\|_{\ell_2(\mathcal{J})} \leq C \|\mathbf{D}_\gamma \mathbf{v}\|_{\ell_2(\mathcal{J})} = C \|v\|_{H(\gamma)}, \quad (4.24)$$

where the constant  $C$  depends only on the constants in (4.6) and (4.8) and is thus independent of  $\gamma$ . Hence  $A(\gamma)$  is uniformly bounded in  $H(\gamma)$  for  $\gamma$  in the resolvent set. This means that the upper estimate in (4.14) holds for  $\mathbf{D}_\gamma^{-1} \mathbf{A}(\gamma) \mathbf{D}_\gamma^{-1}$  with a constant independent of  $\gamma$ . The validity of a lower bound independent of  $|\gamma|$  seems less clear. However, computational evidence shows clearly that scaling by  $\mathbf{D}_\gamma$  is by far superior to scaling by  $\mathbf{D}$ .

Thus we shall employ **Solve** with respect to the scaling  $\mathbf{D}_\gamma$  which will allow us to compute the integrand in (4.1) at certain nodes  $\gamma_k$  within suitable accuracy tolerances. This will be seen to constitute a main ingredient for the numerical application of the operators in (4.1). We shall make frequent use of the following simple facts.

REMARK 4. *Note that for all the above scalings one has  $\mathbf{D}_{\lambda,\lambda} \geq 1$ ,  $(\mathbf{D}_\gamma)_{\lambda,\lambda} \geq 1$ , for all  $\lambda \in \mathcal{J}$ . This implies that for  $w = \mathbf{w}^T \Psi$*

$$\|\mathbf{D}^{-1} \mathbf{w}\|_{\ell_2(\mathcal{J})} \leq \|\mathbf{w}\|_{\ell_2(\mathcal{J})}, \quad \mathbf{w} \in \ell_2(\mathcal{J}), \quad (4.25)$$

which are the discrete analogues of the embedding inequalities

$$\|w\|_V \leq \|w\|_H, \quad \|w\|_V \leq \|w\|_{H(\gamma)}, \quad w \in H. \quad (4.26)$$

**4.2. Applying Projections.** We are now prepared to formulate algorithms for computing the application of the projected semigroup

$$e^{-tA} P_{\Gamma_1} v = \frac{1}{2\pi i} \int_{\Gamma_1} e^{-t\gamma} (\gamma I - A)^{-1} v \, d\gamma, \quad t \in \mathbb{R},$$

or as the special case  $t = 0$ , of the projection

$$P_{\Gamma_1} v = \frac{1}{2\pi i} \int_{\Gamma_1} (\gamma I - A)^{-1} v \, d\gamma,$$

to some fixed  $v \in X$ . We emphasize that in connection with projected semigroups  $t$  may attain negative values as well. We assume that for the Jordan curve  $\Gamma_1$  enclosing some bounded subset of  $\sigma(A)$ , as described in Section 3, an analytic and  $2\pi$ -periodic parameterization

$$s \mapsto \gamma(s), \quad s \in [0, 2\pi),$$

is given. Then, the integrand

$$F(s) = -i\gamma'(s) e^{-t\gamma(s)} (\gamma(s)I - A)^{-1} v, \quad s \in [0, 2\pi),$$

is also  $2\pi$ -periodic and analytic in the topology of  $X$  so that the following theorem applies.

THEOREM 4.1. ([13], Theorem 12.6) *Let  $F : \mathbb{R} \rightarrow X$  be analytic and  $2\pi$ -periodic. Then, there exists  $q > 0$  such that  $F$  extends to an analytic, bounded, and  $2\pi$ -periodic*

function on the strip  $\mathcal{D}_q = \{x + iy : x \in \mathbb{R}, |y| < q\}$ . Moreover, the quadrature error of the trapezoidal rule

$$Q_N(F) = \frac{1}{2N} \sum_{k=0}^{2N-1} F\left(\frac{k\pi}{N}\right), \quad N \in \mathbb{N},$$

is bounded by

$$\left\| \frac{1}{2\pi} \int_0^{2\pi} F(s) ds - Q_N(F) \right\|_X \leq \|F\|_{L_\infty(\mathcal{D}_q, X)} \frac{1}{e^{2qN} - 1}. \quad (4.27)$$

Since we are lacking any estimate for  $q$  and  $\|F\|_{L_\infty(\mathcal{D}_q, X)}$  it seems reasonable to use

$$\|Q_N(F) - Q_{2N}(F)\|_X \approx \|Q_N(F) - e^{-tA} P_{\Gamma_1} v\|_X$$

as error estimator. This is certainly true when (4.27) holds with  $\leq$  replaced by  $\sim$ . To ensure convergence of the upcoming algorithm we therefore make the following

ASSUMPTION 1. *There exist constants  $c_Q, C_Q > 0$  and  $N_0 \geq 1$  such that*

$$c_Q \|Q_N(F) - Q_{2N}(F)\|_X \leq \|Q_N(F) - e^{-tA} P_{\Gamma_1} v\|_X$$

and

$$\|Q_N(F) - e^{-tA} P_{\Gamma_1} v\|_X \leq C_Q \|Q_N(F) - Q_{2N}(F)\|_X$$

for all  $N \geq N_0$ .

Since, as indicated above, the resolvents in (4.1) will be applied in the wavelet coordinate domain, we shall derive next the wavelet representation of the projected semigroup. We shall assume in what follows  $X = V = Y$ , see (2.21). Since the resolvents apply to elements in  $H'$  which are naturally expanded in terms of the dual basis  $\tilde{\Psi}$  we choose to represent  $e^{-tA} P_{\Gamma_1}$  with respect to  $\tilde{\Psi}$ , i.e. we set

$$\mathbf{PE}(t) = \langle \tilde{\Psi}, e^{-tA} P_{\Gamma_1} \tilde{\Psi} \rangle, \quad \text{i.e. } e^{-tA} P_{\Gamma_1} v = (\mathbf{PE}(t) \mathbf{v})^T \tilde{\Psi}. \quad (4.28)$$

To formulate the following algorithm, we define  $N_l = 2^l N_0$ ,  $l \in \mathbb{N}$ . The quadrature points associated with  $N_l$  are  $s_{l,k} = \frac{k\pi}{N_l}$ ,  $k = 0, 1, \dots, 2N_l - 1$ . Obviously, the sequences of quadrature points are nested, i.e.  $s_{l+1,2k} = s_{l,k}$ . Therefore,  $Q_{N_l}(F)$  can be improved to  $Q_{2N_l}(F)$  by evaluating the integrand  $F$  at the nodes  $s_{l+1,2k+1}$ ,  $k = 0, 1, \dots, N_l - 1$ .

ALGORITHM 1.  $\mathbf{w} \leftarrow \mathbf{Apply}(\mathbf{PE}(t), \eta, \mathbf{v})$

- Fix some  $0 < \varrho \leq \frac{c_R}{3C_Q C_R}$ .
- For  $k = 0, 1, \dots, 2N_0 - 1$

$$\mathbf{w}_{0,k} \leftarrow \mathbf{Solve}(\mathbf{D}_{\gamma(s_{0,k})}, \mathbf{A}(\gamma(s_{0,k})), \frac{\eta \min\{1, \frac{3}{2}\varrho\}}{3|\gamma'(s_{0,k}) \exp(-t\gamma(s_{0,k}))|}, \gamma(s_{0,k})^{-1} \mathbf{v})$$

- $\mathbf{w}_0 \leftarrow \frac{-i}{2N_0} \sum_{k=0}^{2N_0-1} \gamma'(s_{0,k}) e^{-t\gamma(s_{0,k})} \mathbf{w}_{0,k}$
- For  $l = 1, 2, \dots$

– for  $k = 1, 3, \dots, 2N_l - 1$

$$\mathbf{w}_{l,k} \leftarrow \mathbf{Solve}(\mathbf{D}_{\gamma(s_{l,k})}, \mathbf{A}(\gamma(s_{l,k})), \frac{\eta \min\{1, \frac{3}{2}\varrho\}}{3|\gamma'(s_{l,k}) \exp(-t\gamma(s_{l,k}))|}, \gamma(s_{l,k})^{-1} \mathbf{v})$$

- $\mathbf{u}_l \leftarrow \frac{-i}{2N_l} \sum_{k=0}^{N_l-1} \gamma'(s_{l,2k+1}) e^{-t\gamma(s_{l,2k+1})} \mathbf{w}_{l,2k+1}$
- $\mathbf{d}_l \leftarrow \frac{1}{2} \mathbf{w}_{l-1} - \mathbf{u}_l$



- $\mathbf{w}_l \leftarrow \frac{1}{2}(\mathbf{w}_{l-1} + \mathbf{u}_l)$
- If  $\|\mathbf{d}_l\|_{\ell_2(\mathcal{J})} \leq \varrho\eta$  then return  $\mathbf{w} = \mathbf{w}_{l-1}$ .

REMARK 5. To remain consistent with the theory the algorithm returns  $\mathbf{w}_{l-1}$ . In practice,  $\mathbf{w}_l$  should be returned as it is the more accurate approximation. Note that the output is given as the array of wavelet coefficients with respect to the basis  $\Psi$  of  $V$ .

LEMMA 4.2. If assumption 1 holds the algorithm **Apply**( $\mathbf{PE}(t), \eta, \mathbf{v}$ ) terminates after a finite number of steps for every  $\eta > 0$  and its output  $\mathbf{w}$  satisfies

$$\|\mathbf{w} - \mathbf{PE}(t)\mathbf{v}\|_{\ell_2(\mathcal{J})} \leq \eta.$$

*Proof.* Let  $\widehat{\mathbf{w}}_{l,k}$  denote the exact solution of

$$\mathbf{A}(\gamma(s_{l,k}))\widehat{\mathbf{w}}_{l,k} = \gamma(s_{l,k})^{-1}\mathbf{v},$$

and define  $\widehat{\mathbf{u}}_l$ ,  $\widehat{\mathbf{d}}_l$  and  $\widehat{\mathbf{w}}_l$  as the corresponding quantities from the algorithm. According to the error bounds guaranteed by **Solve** we have

$$\begin{aligned} & \|\mathbf{w}_{l-1} - \widehat{\mathbf{w}}_{l-1}\|_{\ell_2(\mathcal{J})} \\ & \leq \frac{1}{2N_{l-1}} \sum_{k=0}^{2N_{l-1}-1} |\gamma'(s_{l-1,k})e^{-t\gamma(s_{l-1,k})}| \cdot \|\mathbf{w}_{l-1,k} - \widehat{\mathbf{w}}_{l-1,k}\|_{\ell_2(\mathcal{J})} \\ & \leq \frac{1}{2N_{l-1}} \sum_{k=0}^{2N_{l-1}-1} \frac{\eta}{3} \min\{1, \frac{3}{2}\varrho\} \leq \frac{1}{3}\eta \min\{1, \frac{3}{2}\varrho\}, \end{aligned}$$

where we have used (4.18) and (4.25).

Similarly one obtains

$$\|\mathbf{u}_l - \widehat{\mathbf{u}}_l\|_{\ell_2(\mathcal{J})} \leq \frac{1}{6}\eta \min\{1, \frac{3}{2}\varrho\}, \quad \|\mathbf{d}_l - \widehat{\mathbf{d}}_l\|_{\ell_2(\mathcal{J})} \leq \frac{1}{3}\eta \min\{1, \frac{3}{2}\varrho\}.$$

First, the termination criterion is shown to be met for sufficiently large  $l \in \mathbb{N}$ . From Theorem 4.1 and Assumption 1 the estimate

$$\begin{aligned} \|\mathbf{d}_l\|_{\ell_2(\mathcal{J})} & \leq \|\widehat{\mathbf{d}}_l\|_{\ell_2(\mathcal{J})} + \|\mathbf{d}_l - \widehat{\mathbf{d}}_l\|_{\ell_2(\mathcal{J})} \\ & \leq (c_R c_Q)^{-1} \|F\|_{L^\infty(\mathcal{D}_q, H)} \frac{1}{e^{2dN_l} - 1} + \frac{1}{2}\varrho\eta \end{aligned}$$

follows. Since the first summand tends to zero for  $l \rightarrow \infty$  there exist  $l_0 \in \mathbb{N}$  such that the termination criterion  $\|\mathbf{d}_{l_0}\| \leq \varrho\eta$  is indeed met.

In a second step, the error bound is shown to hold for  $\mathbf{w} = \mathbf{w}_{l_0-1}$ . Obviously, one has

$$\begin{aligned} & \|\mathbf{w}_{l_0-1} - \langle \widetilde{\Psi}, e^{-tA} P_\Gamma v \rangle\|_{\ell_2(\mathcal{J})} \\ & \leq \|\mathbf{w}_{l_0-1} - \widehat{\mathbf{w}}_{l_0-1}\|_{\ell_2(\mathcal{J})} + \|\widehat{\mathbf{w}}_{l_0-1} - \langle \widetilde{\Psi}, e^{-tA} P_\Gamma \widetilde{\Psi} \rangle \mathbf{v}\|_{\ell_2(\mathcal{J})} \\ & \leq \frac{1}{3}\eta + \|\widehat{\mathbf{w}}_{l_0-1} - \langle \widetilde{\Psi}, e^{-tA} P_\Gamma \widetilde{\Psi} \rangle \mathbf{v}\|_{\ell_2(\mathcal{J})}. \end{aligned}$$

The second summand is bounded with the aid of the norm equivalences (4.8) and Assumption 1,

$$\begin{aligned}
\|\widehat{\mathbf{w}}_{l_0-1} - \langle \widetilde{\Psi}, e^{-tA} P_{\Gamma} v \rangle\|_{\ell_2(\mathcal{J})} &\leq c_R^{-1} \|Q_{N_{l_0-1}}(F) - e^{-tA} P_{\Gamma} v\|_H \\
&\leq c_R^{-1} C_Q \|Q_{N_{l_0-1}}(F) - Q_{N_{l_0}}(F)\|_H \\
&\leq c_R^{-1} C_R C_Q \|\widehat{\mathbf{w}}_{l_0-1} - \widehat{\mathbf{w}}_{l_0}\|_{\ell_2(\mathcal{J})} \\
&\leq c_R^{-1} C_R C_Q \left( \|\mathbf{d}_{l_0}\|_{\ell_2(\mathcal{J})} + \|\widehat{\mathbf{d}}_{l_0} - \mathbf{d}_{l_0}\|_{\ell_2(\mathcal{J})} \right). \quad (4.29)
\end{aligned}$$

Since the termination criterion is met the first summand in the brackets is bounded by

$$\|\mathbf{d}_{l_0}\|_{\ell_2(\mathcal{J})} \leq \rho\eta \leq \frac{c_R}{C_Q C_R} \frac{\eta}{3}.$$

The second one can be estimated by

$$\|\widehat{\mathbf{d}}_{l_0-1} - \mathbf{d}_{l_0-1}\|_{\ell_2(\mathcal{J})} \leq \frac{1}{2} \varrho\eta \leq \frac{c_R}{C_Q C_R} \frac{\eta}{4}.$$

Inserting both estimates in (4.29) yields

$$\|\widehat{\mathbf{w}}_{l_0-1} - \langle \widetilde{\Psi}, e^{-tA} P_{\Gamma} v \rangle\|_{\ell_2(\mathcal{J})} \leq \frac{2}{3} \eta.$$

Thus, the overall error of the output  $\mathbf{w}$  is bounded by  $\eta$ .  $\square$

It should be noted that the explicit knowledge of the constant  $c_Q$  is not needed in the algorithm. Its existence is merely needed to show that the algorithm terminates (i.e. it is actually an algorithm).

Since the constants in the quadrature rule are not numerically accessible, one might think of extrapolation techniques to overcome this handicap. But extrapolation is useless for analytic periodic functions since all constants in the asymptotic error expansion of the trapezoidal rule vanish.

**REMARK 6.** *One could also view  $e^{-tA} P_{\Gamma_1}$  as a mapping from  $H'$  to  $H$  (corresponding to the choice  $X = H', Y = H$ ) which would require controlling the error in  $H$ . This can be facilitated by applying **Solve** not with the  $\gamma$ -adapted scaling  $\mathbf{D}_{\gamma}$  but just with the  $H$ -scaling  $\mathbf{D}$  and replacing the constants  $c_R, C_R$  by  $c_H, C_H$ , respectively. According to (4.18), the results of solve satisfy the required bounds now in  $H$ . However, the computational work would increase due to smaller error reduction per iteration step caused by the possibly very large ratios  $C_{A(\gamma)}/c_{A(\gamma)}$  in (4.5).*

**5. Approximate Regularized Inversion of  $e^{-tA}$ .** We shall show next how to use the tools developed in the preceding section in order to regularize the inversion of the operator  $S = e^{-tA}$  for some fixed time  $t > 0$ . Since  $S$  is one-to-one and compact the operator fulfills the assumptions made in Section 2. We shall work in the setting (2.21).

We shall develop three different approaches for regularization according to the strategies (2.13), (2.16) and (3.4). The first approach uses regularization in function spaces, based on the Tikhonov or modified Tikhonov principle (2.13), (2.16), while the resulting operator equations are solved in the wavelet coordinate domain. The second strategy, which is briefly sketched only for the plain Tikhonov scheme, places also the regularization in the wavelet coordinate domain. The third strategy based on

(3.4) is quite different and relies on the inversion of projected semigroups according to Proposition 3.3 and is directly based on the evaluation scheme shown above.

In analogy to (4.28), the corresponding representations of  $S = e^{-tA}$  is given by

$$\mathbf{E}(t) := \langle \tilde{\Psi}, e^{-tA} \tilde{\Psi} \rangle. \quad (5.1)$$

We note that approximate evaluation schemes

$$\mathbf{Apply}(\mathbf{E}(t), \bar{\mathbf{v}}, \eta), \quad (5.2)$$

has a completely analogous structure using trapezoidal quadrature for the Dunford integral

$$e^{-tA}v = \frac{1}{2\pi i} \int_{\Gamma} e^{-t\gamma} (\gamma I - A)^{-1} d\gamma, \quad t \geq 0,$$

defined for sectorial operators. Here the open curve  $\Gamma$  is to enclose the whole spectrum of  $A$  in a proper way. For a detailed discussion and analysis of such evaluation schemes we refer to [15, 16, 11]. Alternatively, in view of Remark 2, we could realize the scheme  $\mathbf{Apply}(\mathbf{E}(t), \bar{\mathbf{v}}, \eta)$  with the aid of Algorithm 1 combined with a proper choice of the curve  $\Gamma_1$ . Therefore, we shall assume that the scheme in (5.2) is given, while its specific realization will not matter.

As for a proper scaling, note that in the context of Tikhonov type regularization (2.13) the operator  $\alpha I + S^*S$  is a norm isomorphism of  $V$  (although its condition number behaves like  $\alpha^{-1}$  when  $\alpha$  gets small). Furthermore, note that either version outputs coefficient arrays with respect to the dual basis  $\tilde{\Psi}$ . While this is justified by the nature of  $S$  it has some practical drawbacks. In fact, in practical constructions the primal basis  $\Psi$  is typically piecewise polynomial and comfortable routines are available for further manipulating or processing the approximate solutions. The dual basis  $\tilde{\Psi}$  is typically less regular and less convenient to handle. Therefore, we indicate next briefly how to switch representations with the aid of numerically executable Riesz maps. Clearly, expanding the  $\psi_\lambda$  in terms of the  $\tilde{\psi}_\lambda$ , yields

$$\Psi = \langle \Psi, \Psi \rangle \tilde{\Psi} \quad \text{i.e.} \quad \mathbf{I} = \langle \Psi, \Psi \rangle \langle \tilde{\Psi}, \tilde{\Psi} \rangle. \quad (5.3)$$

Thus, defining the Gramian  $\mathbf{G} = \langle \tilde{\Psi}, \tilde{\Psi} \rangle$ , we have

$$\bar{\mathbf{v}}^T \Psi = (\mathbf{G} \bar{\mathbf{v}})^T \tilde{\Psi}, \quad (5.4)$$

i.e. application of the Gramian to primal coordinates yields the dual coordinates. Likewise, since  $\mathbf{I} = \langle \Psi, \tilde{\Psi} \rangle$ , we obtain for any endomorphism  $B$  of  $V$

$$\langle \Psi, B\Psi \rangle = \langle \Psi, \Psi \rangle \langle \tilde{\Psi}, B\tilde{\Psi} \rangle \langle \tilde{\Psi}, \tilde{\Psi} \rangle = \mathbf{G} \langle \tilde{\Psi}, B\tilde{\Psi} \rangle \mathbf{G}. \quad (5.5)$$

**5.1. Tikhonov-Type Schemes.** According to (2.13) and (2.16), and recalling that  $A$  is assumed to be normal, the (modified) Tikhonov regularization requires, in view of (3.2), solving the operator equation

$$(\alpha Q_\alpha + e^{-tB})x = e^{-tA^*}y, \quad B := A^* + A, \quad (5.6)$$

Concerning an equivalent formulation in wavelet coordinates, recall that the resolvent application suggested to represent the evolution operators in the dual basis  $\tilde{\Psi}$ , i.e.

$$\mathbf{Q}_\alpha = \langle \tilde{\Psi}, Q_\alpha \tilde{\Psi} \rangle, \quad \mathbf{E}^B(t) = \langle \tilde{\Psi}, e^{-tB} \tilde{\Psi} \rangle, \quad (5.7)$$

where  $Q_\alpha$  either denotes the identity or a projection, depending on the size of  $\alpha$ . Here we use the superscript  $B$  to distinguish  $\mathbf{E}^B(t)$  from the representation  $\mathbf{E}(t)$  of the original semigroup  $e^{-tA}$ . If we were content with representing the solution  $x$  in dual coordinates  $x = \tilde{x}^T \tilde{\Psi}$ , (5.6) is equivalent to

$$(\alpha \mathbf{Q}_\alpha + \mathbf{E}^B(t)) \tilde{\mathbf{x}} = \langle \Psi, e^{-tA^*} y \rangle = \mathbf{E}(t)^* \langle \Psi, y \rangle. \quad (5.8)$$

If, as argued above, we wish to represent  $x = \mathbf{x}^T \Psi \in V$  in primal coordinates we obtain, on account of (5.5), the alternate equivalent formulation

$$\mathbf{G} (\alpha \mathbf{Q}_\alpha + \mathbf{E}^B(t)) \mathbf{G} \mathbf{x} = \mathbf{G} \mathbf{E}^*(t) \langle \Psi, y \rangle. \quad (5.9)$$

(5.8) would save two applications of  $\mathbf{G}$  per iteration step in comparison with (5.9). Of course, one could transform at the end  $\tilde{\mathbf{x}}$  into primal coordinates by applying the inverse  $\mathbf{G}^{-1} = \langle \tilde{\Psi}, \tilde{\Psi} \rangle$ . But the latter one is usually less compressible rendering its application less efficient. Therefore we concentrate in what follows on (5.9).

We wish to solve the system (5.9) within any desired target accuracy with the aid of the scheme **Solve** following the lines of [2]. The main building blocks are algorithms to apply the involved operators up to any prescribed accuracy. We provide these ingredients in the following subsections. The above representations involve, in particular, the (infinite) matrix  $\mathbf{G}$ . The vanishing moment property of wavelets allows one to apply  $\mathbf{G}$  to any finitely supported vector within any prescribed accuracy tolerance by the schemes developed in [2, 1]. Moreover, within a certain basis dependent range such an application has asymptotically optimal complexity in the sense described earlier. Such a multiplication scheme is also a central building block in the scheme **Solve** and will be denoted by  $\mathbf{Mult}(\mathbf{G}, \eta, \mathbf{v}) \rightarrow \mathbf{w}_\eta$  providing an approximation  $\mathbf{w}_\eta$  to  $\mathbf{G} \mathbf{v}$  such that  $\|\mathbf{G} \mathbf{v} - \mathbf{w}_\eta\|_{\ell_2(\mathcal{J})} \leq \eta$ .

**5.1.1. The Right Hand Side  $\mathbf{z}$ .** Let  $\mathbf{y} = \langle \Psi, y \rangle \in \ell_2(\mathcal{J})$  be given. Then the right hand side of (5.9) has the representation

$$\mathbf{z} = \langle \Psi, e^{-tA^*} y \rangle = \langle \Psi, \Psi \rangle \langle \tilde{\Psi}, e^{-tA^*} \tilde{\Psi} \rangle \mathbf{y} = \mathbf{G} \mathbf{E}^*(t) \mathbf{y}.$$

As  $\mathbf{y}$  has possibly infinitely many non-vanishing entries the following scheme starts formally with a coarsening step to approximate  $\mathbf{y}$  by a finite dimensional vector, see [2] for details concerning the routine **Coarse**  $(\eta, \mathbf{v}) \rightarrow \mathbf{v}_\eta$  such that  $\|\mathbf{v} - \mathbf{v}_\eta\|_{\ell_2(\mathcal{J})} \leq \eta$  and  $\mathbf{v}_\eta$  has (near) minimal support. In practice, an approximation of  $\mathbf{y}$  with accuracy  $\eta_1$  should be calculated in the first step.

ALGORITHM 2.  $\mathbf{w} \leftarrow \mathbf{EvalRhs}(\eta, \mathbf{y})$

- $\mathbf{w}_1 \leftarrow \mathbf{Coarse}(\eta_1, \mathbf{y}),$   $\eta_1 = \frac{c_R^2}{3C_R^2 \|e^{-tA^*}\|_{\mathcal{L}(V)}} \eta;$
- $\mathbf{w}_2 \leftarrow \mathbf{Apply}(\mathbf{E}^*(t), \eta_2, \mathbf{w}_1),$   $\eta_2 = \frac{\eta}{3C_R^2};$
- $\mathbf{w} \leftarrow \mathbf{Mult}(\mathbf{G}, \eta_3, \mathbf{w}_2),$   $\eta_3 = \frac{\eta}{3}.$

LEMMA 5.1. *The output  $\mathbf{w}$  of  $\mathbf{EvalRhs}(\eta, \mathbf{y})$  satisfies*

$$\|\langle \Psi, e^{-tA^*} \Psi \rangle \mathbf{y} - \mathbf{w}\|_{\ell_2(\mathcal{J})} \leq \eta.$$

*Proof.* Repeated application of the triangle inequality yields

$$\begin{aligned} & \|\langle \Psi, e^{-tA^*} y \rangle - \mathbf{w}\|_{\ell_2(\mathcal{J})} \\ & \leq \|\mathbf{G}\|_{\mathcal{L}(\ell_2(\mathcal{J}))} (\|\mathbf{E}^*(t)\|_{\mathcal{L}(\ell_2(\mathcal{J}))} \cdot \eta_1 + \eta_2) + \eta_3. \end{aligned}$$

As, by remark 3,  $\|\mathbf{G}\|_{\mathcal{L}(\ell_2(\mathcal{J}))} \leq C_R^2$  and  $\|\mathbf{E}^*(t)\|_{\mathcal{L}(\ell_2(\mathcal{J}))} \leq c_R^{-2} \|e^{-tA^*}\|_{\mathcal{L}(V)}$ , the choice of  $\eta_1, \eta_2$ , and  $\eta_3$  ensures that the error is bound by  $\eta$ .  $\square$

**5.1.2. The Projection.** Given a regularization parameter  $\alpha > 0$  the orthogonal projection  $Q_\alpha$  onto the eigenspace associated with the eigenvalues of  $e^{-tA^*} e^{-tA} = e^{tB}$ , in  $[0, \alpha]$  is to be evaluated. Denote by  $\{\lambda_k\}_{k \geq 1}$  the eigenvalues of  $B = A + A^*$  sorted by increasing size,  $\lambda_k \leq \lambda_{k+1}$ . Due to the spectral mapping theorem 3.1 we have

$$\begin{aligned} \sigma(e^{-tB}) \cap [0, \alpha] &= (\{0\} \cup \{e^{-t\lambda_k} : k \geq 1\}) \cap [0, \alpha] \\ &= \{0\} \cup \{e^{-t\lambda_k} : \lambda_k \geq \frac{1}{t} \log(\frac{1}{\alpha})\}. \end{aligned}$$

By the results of Section 3 we are capable to evaluate projections onto the eigenspaces associated to any bounded subset of  $\sigma(B)$ . Thus, the representation  $Q_\alpha = I - P_\alpha$  is used where  $P_\alpha = P_{\Gamma_1}(B)$  and the Jordan curve  $\Gamma_1$  encloses  $\{\lambda_k : \lambda_k < \frac{1}{t} \log(\frac{1}{\alpha})\}$  (cf. Section 3). The representation of  $Q_\alpha$  with respect to  $\Psi$  becomes

$$\langle \Psi, Q_\alpha \Psi \rangle = \mathbf{G}(I - \mathbf{P}_\alpha)\mathbf{G},$$

where  $\mathbf{P}_\alpha = \mathbf{P}\mathbf{E}(0)$  is the projection in wavelet coordinates.

**5.1.3. The Operator**  $e^{-tA^*} e^{-tA} = e^{-tB}$ . The observations in Section 5.1, suggest the following algorithm to evaluate  $\langle \Psi, (\alpha I + e^{-tB}) \Psi \rangle \mathbf{v} = \mathbf{G}(\alpha I + \mathbf{E}^B(t))\mathbf{G}\mathbf{v}$ , where  $\mathbf{v}$  are here the expansion coefficients with respect to the basis  $\Psi$  of  $V$ .

ALGORITHM 3.  $\mathbf{w} \leftarrow \mathbf{Apply}(\langle \Psi, (\alpha I + e^{-tB}) \Psi \rangle, \eta, \mathbf{v})$

- $\mathbf{w}_1 \leftarrow \mathbf{Mult}(\mathbf{G}, \eta_1, \mathbf{v}),$   $\eta_1 = \frac{c_R^2}{3C_R^2 \|e^{-tB}\|_{\mathcal{L}(V)}} \eta;$
- $\mathbf{w}_2 \leftarrow \mathbf{Apply}(\mathbf{E}^B(t), \eta_2, \mathbf{w}_1),$   $\eta_2 = \frac{1}{3C_R^2} \eta;$
- $\mathbf{w} \leftarrow \mathbf{Mult}(\mathbf{G}, \eta_3, \alpha \mathbf{v} + \mathbf{w}_2),$   $\eta_3 = \frac{1}{3} \eta.$

Clearly, in the third step we invoke Algorithm 1. An analogous reasoning as in the proof of Lemma 5.1 yields the following estimate.

LEMMA 5.2. *The output  $\mathbf{w}$  of  $\mathbf{Apply}(\langle \Psi, (\alpha I + e^{-tB}) \Psi \rangle, \eta, \mathbf{v})$  satisfies*

$$\|\langle \Psi, (\alpha I + e^{-tB}) \Psi \rangle - \mathbf{w}\|_{\ell_2(\mathcal{J})} \leq \eta.$$

If the identity is replaced by a projection  $Q_\alpha = I - P_\alpha$  a similar algorithm is used where in addition Algorithm 1 is called.

ALGORITHM 4.  $\mathbf{w} \leftarrow \mathbf{Apply}(\langle \Psi, (\alpha Q_\alpha + e^{-tB}) \Psi \rangle, \eta, \mathbf{v})$

- $\mathbf{w}_1 \leftarrow \mathbf{Mult}(\mathbf{G}, \eta_1, \mathbf{v}),$   $\eta_1 = \frac{c_R^2}{4C_R^2 (\alpha + \|e^{-tB}\|_{\mathcal{L}(V)})} \eta;$
- $\mathbf{w}_2 \leftarrow \mathbf{Apply}(\mathbf{E}^B(t), \eta_2, \mathbf{w}_1),$   $\eta_2 = \frac{1}{4C_R^2} \eta;$
- $\mathbf{w}_3 \leftarrow \mathbf{Apply}(\langle \tilde{\Psi}, P_\alpha \tilde{\Psi} \rangle, \eta_3, \mathbf{w}_1),$   $\eta_3 = \frac{1}{4\alpha C_R^2} \eta;$
- $\mathbf{w} \leftarrow \mathbf{Mult}(\mathbf{G}, \eta_4, \alpha(\mathbf{v} - \mathbf{w}_3) + \mathbf{w}_2),$   $\eta_4 = \frac{1}{4} \eta.$

A similar proof as in Lemma 5.1 yields the following estimate.

LEMMA 5.3. *The output  $\mathbf{w}$  of  $\mathbf{Apply}(\langle \Psi, (\alpha Q_\alpha + e^{-tB}) \Psi \rangle, \eta, \mathbf{v})$  satisfies*

$$\|\langle \Psi, (\alpha Q_\alpha + e^{-tB}) \Psi \rangle - \mathbf{w}\|_{\ell_2(\mathcal{J})} \leq \eta.$$

We have prepared now all the algorithmic ingredients needed to apply the scheme **Solve** from [2] to the operator equation (5.6) which will return an approximate solution  $x_\eta$  that approximates  $x$  with accuracy  $\eta$ .

**5.2. The Discrepancy Principle.** With the wavelet representations of the operators at hand, we can formulate a version of the discrepancy principle for the above Tikhonov-type schemes. The following algorithm is based on Lemma 2.3. We assume that the three parameters  $\tau, \tau_1, \tau_2 > 0$  are given such that  $\tau - \tau_1 - \tau_2 > 1$  holds (cf. (2.10)). Moreover, we fix  $c \in [1/2, 1)$  and test the stopping criterion

$$\|Sx_{\alpha_{k+1}} - y^\delta\|_V \leq \tau\delta \leq \|Sx_{\alpha_k}^\delta - y^\delta\|_V$$

for  $\alpha_k = c^k \alpha_0$ . Recall that we have here  $V = X = Y$ . The choice of  $c$  permits a certain tuning of the algorithm, as the search for the optimal  $\alpha$  becomes more thorough and more expensive for  $c$  closer to one. By the previous remarks, the scaling in **Solve** is just the identity.

ALGORITHM 5.  $\mathbf{x} \leftarrow \mathbf{DiscrepancyPrinciple}(y^\delta, \delta, \alpha_0)$

For  $k = 0, 1, \dots$

- $\alpha_k := c^k \alpha_0$
- $\mathbf{x}_k \leftarrow \mathbf{Solve}(\mathbf{I}, \langle \Psi, (\alpha_k Q_{\alpha_k} + S^* S) \Psi \rangle, \tau_1 \|S\|^{-1} \delta, y^\delta)$
- $\mathbf{w}_k \leftarrow \mathbf{Apply}(\langle \Psi, S \Psi \rangle, \mathbf{x}_k, \frac{1}{2} \tau_2 \delta)$
- $\mathbf{r}_k \leftarrow \mathbf{w}_k - \mathbf{EvalRhs}(\frac{1}{2} \tau_2 \delta, y^\delta)$
- If  $\|\mathbf{r}_k\|_{\ell_2(\mathcal{J})} \leq \tau\delta$  then return  $\mathbf{x} \leftarrow \mathbf{x}_k$ .

THEOREM 5.4. *The algorithm **DiscrepancyPrinciple** defines a regularization scheme of optimal order for  $0 < \mu \leq 1/2$ . More precisely, the output  $x = \mathbf{x}^T \Psi$  of **DiscrepancyPrinciple**( $y^\delta, \delta, \alpha_0$ ) satisfies*

$$\|x - x^\dagger\|_V \leq C \delta^{\frac{2\mu}{2\mu+1}} \rho^{\frac{1}{2\mu+1}} \quad (5.10)$$

for all  $y^\delta \in Y$  with  $\|y^\delta - y\|_V \leq \delta$  and all  $x^\dagger = (S^* S)^\mu w$  with  $\|w\|_V \leq \rho$ ,  $0 < \mu \leq 1/2$ .

*Proof.* According to the norm equivalence (4.6) we have

$$\|x - x^\dagger\|_X \sim \|\mathbf{x} - \langle x^\dagger, \tilde{\Psi} \rangle\|_{\ell_2(\mathcal{J})}.$$

Thus it is sufficient to establish (5.10) for  $x - x^\dagger$  in wavelet coordinates. To do so, we rely on Lemma 2.3. From the target accuracy in **Solve**, **Apply**, and **EvalRhs** it is immediate that the conditions (2.8) and (2.9) are satisfied for the wavelet coefficient arrays  $\mathbf{x}_k$  and  $\text{Res}_\alpha = \|\mathbf{r}_k\|_{\ell_2(\mathcal{J})}$ . The algorithm terminates if and only if (2.11) is satisfied. Therefore we infer from Lemma 2.3 the validity of (5.10), recalling that  $\mu_0 = 1$  for the Tikhonov scheme.  $\square$

Recall that usually one approximate application of the Tikhonov operator on the left hand side of (5.6) requires solving a forward and backward evolution equation (aside from the projection  $Q_\alpha$ ). Here such an application is essentially reduced to schemes of the form (5.2) which in turn are based on the parallel solution of resolvent systems. Of course, when  $\alpha$  decreases **Solve** will require an increasing effort for the same target accuracy due to the deteriorating condition of the problem.

**5.3. Regularization of the Transformed Problem.** So far we have first regularized the continuous problem and then transformed it into a well-posed problem in  $\ell_2(\mathcal{J})$  (whose condition, of course, depends on the regularization parameter). In this subsection, we will exchange the order of regularization and transformation. We shall exemplify this briefly only for the Tikhonov method, the modified version being similar. This gives rise to a scheme where norms are easily changed by scaling offering an additional way of influencing the regularization compromise. Accordingly  $X$  and  $Y$  are now different smoothness spaces and no longer coincide with  $V$ .

We consider the problem

$$\mathbf{E}_s(t)\mathbf{x} = \mathbf{y}, \quad (5.11)$$

posed in  $\ell_2(\mathcal{J})$  with the evolution operator given in wavelet coordinates as

$$\mathbf{E}_s(t) = \mathbf{D}^s \langle \tilde{\Psi}, e^{-tA} \tilde{\Psi} \rangle \mathbf{D}^s, \quad s \in [-1, 1],$$

where now  $x = \mathbf{x}^T \mathbf{D}^{-s} \tilde{\Psi}$ . The power  $s$  of the diagonal elements of  $\mathbf{D}$  steers the involved norms. For instance, when  $A$  is a second order elliptic operator,  $\mathbf{E}_0(t) = \mathbf{E}(t)$  is a representation of the operator  $e^{-tA}$  regarded as a mapping  $X = V = \mathbf{L}_2(\Omega) \rightarrow \mathbf{L}_2(\Omega) = Y$ . In general, for  $H = H_0^t(\Omega)$ , it is well-known that the scaling by  $\mathbf{D}^s$  induces equivalent norms on the interpolation spaces between  $H^{-t}(\Omega)$  and  $H_0^t(\Omega)$ , see e.g. [5]. Let us assume here the standard case  $t = 1$ .

As  $e^{-tA}$  is compact the transformed operator has the same property as endomorphism of  $\ell_2(\mathcal{J})$  and the resulting sequence equation is ill-posed, as well. Applying Tikhonov-regularization in  $\ell_2(\mathcal{J})$  yields the equation

$$(\alpha I + \mathbf{E}_s^*(t)\mathbf{E}_s(t))\mathbf{x}_\alpha^\delta = \mathbf{E}_s^*(t)\mathbf{y}^\delta,$$

where  $\mathbf{I}$  denotes again the identity in  $\ell_2(\mathcal{J})$  and not the Gramian matrix.  $\mathbf{y}^\delta$  and  $\mathbf{x}_\alpha^\delta$  are given by

$$\mathbf{y}^\delta = \mathbf{D}^s \langle \Psi, y^\delta \rangle, \quad \mathbf{x}_\alpha^\delta = \mathbf{D}^{-s} \langle \Psi, x_\alpha^\delta \rangle.$$

The regularized equation is equivalent to the solution of the minimization problem

$$\begin{aligned} J_s(\alpha, \mathbf{y}^\delta) &= \alpha \|\mathbf{x}_\alpha^\delta\|_{\ell_2(\mathcal{J})}^2 + \|\mathbf{E}_s(t)\mathbf{x}_\alpha^\delta - \mathbf{y}^\delta\|_{\ell_2(\mathcal{J})}^2 \\ &= \alpha \|\mathbf{D}^{-s} \langle \Psi, x_\alpha^\delta \rangle\|_{\ell_2(\mathcal{J})}^2 + \|\mathbf{D}^s \langle \Psi, e^{-tA} x_\alpha^\delta - y^\delta \rangle\|_{\ell_2(\mathcal{J})}^2 \\ &\rightarrow \min_{\mathbf{x}_\alpha^\delta \in \ell_2(\mathcal{J})}. \end{aligned}$$

By the norm equivalences of the wavelet basis one sees that

$$\|\mathbf{x}_\alpha^\delta\|_{\ell_2(\mathcal{J})} \sim \|x_\alpha^\delta\|_{H^{-s}(\Omega)} \quad \text{and} \quad \|\mathbf{y}^\delta\|_{\ell_2(\mathcal{J})} \sim \|y^\delta\|_{H^s(\Omega)},$$

i.e. we take here  $X = H^{-s}(\Omega)$ ,  $Y = H^s(\Omega)$ . Thus, the smaller  $s$  is the stronger the norm in which smoothness of  $x_\alpha^\delta$  is measured becomes. In turn, the norm in which the residual is measured becomes weaker for smaller  $s$ . In practice, the range  $s \in [-1, 0]$  is of interest as the solution  $x_\alpha^\delta$  should be smooth.

Concerning the convergence of the regularization scheme for  $\delta \rightarrow 0^+$  the properties of Tikhonov regularization read as follows. Suppose that

$$y = e^{-tA} x^\dagger \quad \text{with} \quad x^\dagger \in H^{-s}(\Omega)$$

and

$$\|y - y^\delta\|_{H^s(\Omega)} \leq \delta.$$

Then,

$$\|x_\alpha^\delta - x^\dagger\|_{H^{-s}(\Omega)} \rightarrow 0 \quad \text{for } \delta \rightarrow 0^+,$$

if  $\alpha = \alpha(\delta, y^\delta)$  is chosen properly, e.g. according to the discrepancy principle.

**5.4. Projection Methods.** The third method is quite different and uses the fact that, by Proposition 3.3, the projection of  $S = e^{-tA}$  onto the eigenspaces associated with a bounded subset of  $\sigma(A)$  becomes boundedly invertible.

To fix ideas we assume that  $\sigma(A) = \{\lambda_k : k \in \mathbb{N}\}$  with  $\Re(\lambda_k) \leq \Re(\lambda_{k+1})$  and  $\Re(\lambda_k) \rightarrow \infty$  for  $k \rightarrow \infty$ . Then, by the spectral mapping theorem,  $e^{-tA}$  has the eigenvalues  $e^{-t\lambda_k}$  which tend to zero if  $k \rightarrow \infty$ . Thus, we discard the eigenvalues for large  $k$  by projection. Fix a  $k_0 \in \mathbb{N}$  and set  $\sigma_1 = \{\lambda_k : 1 \leq k \leq k_0\}$ . According to the notation of Section 3, the projection onto the eigenspaces associated with  $\sigma_1$  is denoted by  $P_{\Gamma_1}$ . The projected semigroup  $P_{\Gamma_1}e^{-tA} = e^{-tA_1} : V \rightarrow V$  is boundedly invertible with inverse

$$e^{tA_1} = \frac{1}{2\pi i} \int_{\Gamma_1} e^{t\gamma} (\gamma I - A)^{-1} d\gamma$$

and

$$\|e^{tA_1}\|_{\mathcal{L}(X)} \leq C e^{t\Re(\lambda_{k_0})},$$

for some constant  $C = C(k_0) \geq 1$ . Here we take again  $V = X = Y$ . Thus, the regularized solution defined as

$$x_{k_0}^\delta = e^{tA_1} y^\delta,$$

depends continuously on  $y^\delta$ , and  $1/k_0$  plays the role of the regularization parameter, see (3.4). Clearly, if  $k_0 \rightarrow \infty$  and  $y$  is given exactly the regularized solution  $x_{k_0}$  will tend to  $x^\dagger$  if  $A$  has a complete system of eigenvectors.

When dealing with noisy data,  $k_0$  has to be chosen properly. This can be done again with the aid of the discrepancy principle, i.e. we pick

$$k_0 = \inf\{k \in \mathbb{N} : \|e^{-tA} x_k^\delta - y^\delta\|_V \leq \tau\delta\}$$

for some fixed parameter  $\tau \geq 1$ . Alternatively, the discrepancy principle can be used in the wavelet coordinate domain.

As pointed out at the end of Section 3 the scheme becomes an SVD-projection when  $A$  is selfadjoint and positive definite. We have all the tools at hand to formulate the analogue of Algorithm 5 for the SVD-projection method and also for Theorem 5.4 where, due to  $\mu_0 = \infty$ , the range of the smoothness index  $\mu$  is now unbounded.

Of course, in principle, the projection method is a familiar concept in regularization theory. But, to our knowledge, it has not been implemented yet in the present context with a rigorous error control since the eigenvalues and eigenspaces are in general not numerically accessible. By the techniques developed in [15] and Section 4.2 the scheme becomes for the first time realizable in a fairly general setting.



A rough comparison already indicates that, aside from the fact that higher order regularity can be exploited better, the projection method is computationally more efficient than the Tikhonov scheme. In our setting, for some fixed *positive*  $t > 0$  the algorithm **Apply**( $\mathbf{PE}(-t), \mathbf{y}^\delta, \eta$ ) will be called for some  $\eta \ll \delta$  until the discrepancy principle is met. Each call will need  $N$  elliptic subproblems to be solved within a prescribed tolerance where we observed  $N$  to be well below 80 in our experiments. In contrast, the Tikhonov method requires the solution of the linear system (5.6) for several  $\alpha > 0$ . Any linear solver applied to this problem will perform an application of **Apply**( $\mathbf{E}^B(t), \mathbf{w}, \eta$ ) *once per step* and will need several steps to solve the linear problem. In fact, it will need more and more steps as  $\alpha$  decreases. As **Apply**( $\mathbf{PE}(-t), \mathbf{y}^\delta, \eta$ ) and **Apply**( $\mathbf{E}^B(t), \mathbf{w}, \eta$ ) need at least for small  $t$  roughly the same amount of work the projection method is significantly faster than the Tikhonov scheme.

Of course, it is crucial to come up with suitable curves  $\Gamma_1$  separating the spectrum according to the needs of the discrepancy principle. Moreover, Assumption 1 needs to be validated. These issues will be addressed in Section 6 for a simple test case.

**5.5. Some Comments on Computational Complexity.** Not much seems to be known about the actual computational cost of determining the numerical approximation  $\hat{x}_\alpha^\delta$  for the regularized solution  $x_\alpha^\delta$  depending on the given noise level  $\delta$  as  $\delta$  tends to zero. We address this question now in a somewhat sketchy and partly heuristic way for the simplest scenario that  $A$  is symmetric self adjoint second order elliptic operator so that  $H = H_0^1(\Omega)$ ,  $H' = H^{-1}(\Omega)$ . Hence the singular values  $\sigma_k$  of  $S = e^{-tA}$  are for fixed  $t > 0$  given by  $\sigma_k = e^{-t\lambda_k}$ , where  $\lambda_k$  are the eigenvalues of  $A$ . A detailed rigorous study would be beyond the scope of the present paper and will be given elsewhere. Here we merely wish to bring out what the approach might offer at best and to identify some of the questions along that way.

Let  $\Gamma_1^K$  denote a suitable Jordan curve whose interior contains the first  $K$  eigenvalues  $\lambda_k, k = 1, \dots, K$ . and let  $P_K := P_{\Gamma_1^K}$  be again the projector defined in (3.1). As pointed out before,  $x_K^\delta := e^{tA_1} y^\delta$  with  $e^{-tA_1} = P_K e^{-tA} = e^{-tA} P_K$ , corresponds to a truncated SVD expansion. Since by assumption  $\|P_K(y - y^\delta)\|_V \leq C\delta$  we can invoke [9, Theorem 3.26] to conclude that

$$\|x^\dagger - x_K^\delta\|_V \leq C' \left( \sigma_{K+1} + \frac{\delta}{\sigma_K} \right) \quad (5.12)$$

for some constant  $C'$  independent of  $\delta, K$ . Having some estimates for the  $\lambda_k$  and hence for the  $\sigma_k$ , a reasonable parameter choice is to balance both terms on the right hand side of (5.12). This suggests choosing

$$K = K(\delta) = \max \{k : \sigma_{k+1} \sigma_k \leq \delta\}.$$

In order to retain the accuracy offered by this projection method we compute

$$\hat{x}_K^\delta = \mathbf{x}^T \Psi, \quad \mathbf{x} = \mathbf{Apply}(\mathbf{PE}(-t), \mathbf{y}^\delta, \eta), \quad \text{with } \eta := \delta / \sigma_K. \quad (5.13)$$

Recall that the latter routine is given in Algorithm 1. As before, we do not specify in which form the noisy data  $y^\delta \in V$  are actually given but assume for simplicity that we can observe its wavelet coefficients  $\mathbf{y}^\delta$  for the expansion  $y^\delta = (\mathbf{y}^\delta)^T \tilde{\Psi}$ . Note that by (4.6), we have then

$$\|\mathbf{y} - \mathbf{y}^\delta\|_{\ell_2(\mathcal{J})} \leq c_R^{-1} \delta. \quad (5.14)$$

In this scheme the computational cost is then dominated by the approximate applications of resolvents at quadrature points  $\gamma(s_{l,k})$ ,  $k = 0, \dots, N_l - 1$ ,  $N_l := 2^l N_0$ , on the curve  $\Gamma_1^K$ . By a geometric series argument the overall work is dominated by the quadrature at the terminating level  $L$  of quadrature resolution. For that  $L$  the scheme **Solve** is called  $N_L = 2^L N_0$  times with target accuracies  $\sim \eta/|e^{t\gamma(s_{L,k})}|$ ,  $k = 0, \dots, N_L - 1$ . Thus, the most stringent accuracy constraint is encountered when the real part of  $\gamma(s_{L,k})$  is of the order of  $\lambda_K$ . Hence, a rough bound for the computational cost  $\mathcal{C}_K$  of **Apply** ( $\mathbf{PE}(-t), \mathbf{y}^\delta, \eta$ ) with  $\eta := \delta/\sigma_K$  is given by

$$\mathcal{C}_K \lesssim 2^L N_0 \mathcal{C}(\mathbf{Solve}(\mathbf{D}_{\gamma(s_{L,N_L-1})}, \mathbf{A}(\gamma(s_{L,N_L-1})), c\delta, \gamma(s_{L,N_L-1})^{-1} \mathbf{y}^\delta)), \quad (5.15)$$

where we have used that  $\sigma_K = e^{-t\lambda_K}$  (recall the scaling  $\mathbf{D}_\gamma$  given by (4.19)). Here,  $\mathcal{C}(\mathbf{Solve})$  denotes the computational cost of the routine **Solve** and  $a \lesssim b$  means that  $a$  can be bounded by a fixed multiple of  $b$  which is independent of the parameters on which  $a$  and  $b$  may depend.

It remains now to estimate  $L$  and  $\mathcal{C}(\mathbf{Solve})$  for a target accuracy of the order  $\delta$ . We shall address this latter issue first. Recall that, according to (4.17), **Solve** endowed with the scaling  $\mathbf{D}_\gamma$  operates on right hand side data of the form  $\gamma^{-1} \mathbf{D}_\gamma^{-1} \mathbf{y}^\delta$  which are the expansion coefficients with respect to the  $H(\gamma)'$ -scaled basis  $\mathbf{D}_\gamma \tilde{\Psi}$ . Thus, the noisy input data  $\mathbf{y}^\delta$  are damped in two ways, first by  $\gamma^{-1}$  when  $|\gamma|$  is large, and second, the entries  $y_\lambda^\delta$  for  $|\lambda| \geq \frac{1}{2} \log_2 |\gamma|$  are attenuated by the weights  $(\mathbf{D}_\gamma)_{\lambda,\lambda}^{-1}$ , see (4.19). By (5.14) and (4.25) we also know that

$$\|\gamma^{-1} \mathbf{D}_\gamma^{-1} (\mathbf{y} - \mathbf{y}^\delta)\|_{\ell_2(\mathcal{J})} \leq c_R^{-1} \delta \quad (5.16)$$

uniformly in  $|\gamma| \geq 1$ .

To obtain an impression of  $\mathcal{C}(\mathbf{Solve})$  in this context, suppose now that the exact wavelet coefficient array  $\mathbf{y}$  of  $u(t) = y = \mathbf{y}^T \tilde{\Psi}$  is sparse in the sense that

$$y \in \mathcal{A}^r(V) \quad (5.17)$$

for some  $r > 0$ , i.e. the error of best  $N$ -term approximation in  $\ell_2(\mathcal{J})$  decays like  $N^{-r} |y|_{\mathcal{A}^r(V)}$ . By (4.25), we also have then that

$$\bar{y} := (\mathbf{D}_{\gamma(s)}^{-1} \mathbf{y})^T \tilde{\Psi} \in \mathcal{A}^r(H(\gamma)) \quad (5.18)$$

for that  $r > 0$  and any point  $\gamma(s)$  on  $\Gamma_1^K$  which will actually hold uniformly in  $s$  and  $K$ . We shall explain later what this means in terms of the regularity of  $y$ . Now suppose further that the operator  $A$  and its shifted versions  $A(\gamma(s))$  permit the following ‘‘regularity’’ result:

**ASSUMPTION 2.** *Given a right hand side such that its coefficient array with respect to  $\mathbf{D}_{\gamma(s)} \tilde{\Psi}$  belongs to  $\mathcal{A}^r$  then the solution  $v \in H(\gamma(s))$  has a coefficient array with respect to  $\mathbf{D}_{\gamma(s)}^{-1} \tilde{\Psi}$  which also belongs to  $\mathcal{A}^r$  for some  $r < r^*$  with  $r^*$  the fixed compressibility limit depending on the wavelet bases (see [2, 17]).*

Then, if (4.23) was true, the results in [2] would assert that

$$\mathcal{C}(\mathbf{Solve}(\mathbf{B}(\gamma(s_{L,N_L-1})), c\delta, \bar{y})) \lesssim \delta^{-1/r} |v|_{\mathcal{A}^r}^{1/r}. \quad (5.19)$$

However, **Solve** ‘‘sees’’ only the perturbed data  $\bar{\mathbf{y}}^\delta := \mathbf{D}_{\gamma(s)}^{-1} \mathbf{y}^\delta$ . We dispense here introducing a statistical model and try to construct an estimator reflecting the sparseness of the exact data with high probability or in expectation. Instead we resort to a more

heuristic reason why under the above assumptions one may still obtain a work count like (5.19). This requires a somewhat closer look at the way **Solve** works, see [2]. First of all the data  $\bar{\mathbf{y}}^\delta$  can be considered as a finite array, since every coefficient  $\bar{\mathbf{y}}_\lambda^\delta$  with  $(\mathbf{D}_{\gamma(s)})_{\lambda,\lambda} \leq \delta$  can be discarded which, in view of (5.14), introduces only an error of the order at most  $\delta$  in  $\ell_2(\mathcal{J})$  for the scaled right hand side (which is what matters for **Solve**). Let us call this finite array again  $\bar{\mathbf{y}}^\delta$ . Thus, by (5.16), we still have that  $\|\bar{\mathbf{y}} - \bar{\mathbf{y}}^\delta\|_{\ell_2(\mathcal{J})} \leq C\delta$  for some finite constant  $C$ . Now, given some target accuracy  $\varepsilon$  for **Solve**, the right hand side data are approximated first by a possibly small array within a tolerance  $a\varepsilon$  where  $a$  is typically smaller than one. This approximation is done by a routine **Coarse** described e.g. in [2], see also Section 5.1.1. If we relax our target accuracy  $c\delta$  in **Solve** by some constant factor larger than one, the coarsening of the right hand side data  $\bar{\mathbf{y}}^\delta$  would have to be done with a target accuracy  $bC\delta$  where  $b$  is now any fixed number *larger* than one. But then the Coarsening Lemma from [2] states that the resulting approximation  $\mathbf{y}^*$  to  $\bar{\mathbf{y}}^\delta$  now satisfies

$$\|\bar{\mathbf{y}} - \mathbf{y}^*\|_{\ell_2(\mathcal{J})} \leq (1+b)C\delta, \quad \#\text{supp } \mathbf{y}^* \lesssim \delta^{-1/r} |\bar{\mathbf{y}}|_{\mathcal{A}^s(H(\gamma))}^{1/r}, \quad |\bar{\mathbf{y}}^*|_{\mathcal{A}^r(H(\gamma))} \lesssim |\bar{\mathbf{y}}|_{\mathcal{A}^r(H(\gamma))}. \quad (5.20)$$

Thus, using a fixed but sufficiently large multiple of  $\delta$  as target accuracy in **Solve** the corresponding coarsening of the data that “peels” off at this level of accuracy the sparsity of the exact array  $\bar{\mathbf{y}}$  in the neighborhood. In that sense the routine **Solve** still “sees”  $\bar{\mathbf{y}}$  and exploits its compressibility giving the work count (5.19).

Let us briefly comment now on the above assumptions around (5.18). We wish to recover the initial data  $x^\dagger = u(0) = (\mathbf{x}^\dagger)^T \Psi$  from the data  $y^\delta$ . Suppose that  $u(0) \in B_P^r(L_p(\Omega))$  where  $\frac{1}{p} = \frac{r}{d} + \frac{1}{2}$ . The space  $B_P^r(L_p(\Omega))$  is just embedded in  $L_2(\Omega)$  and signifies in some sense the largest space of smoothness  $r$  contained in  $L_2(\Omega)$ . Note that the larger  $r$  the smaller  $p$  and the weaker the measure for smoothness. It is well known that  $x^\dagger \text{ in } B_P^r(L_p(\Omega))$  implies  $\mathbf{x}^\dagger \in \mathcal{A}^r$ , see e.g. [8]. Moreover, it is known that then  $y = u(t) = e^{-tA}u(0)$  belongs also to  $B_P^r(L_p(\Omega))$ , see [16]. Assumption 2 then says that the assumed gain in regularity through the application of  $A(\gamma(s))^{-1}$  suffices to ensure that the solution array with respect to  $\mathbf{D}_{\gamma(s)}^{-1}\Psi$  is still in  $\mathcal{A}^r$ . For moderate  $|\gamma(s)| \sim 1$  this is simply a regularity theorem for  $A$  itself. For  $A$  as above we would have  $v = A(\gamma(s))^{-1}y \in B_P^{r+2}(L_p(\Omega))$ . Note that already  $v \in B_P^{r+1}(L_p(\Omega))$  would suffice to ensure that for  $v = \mathbf{v}^T \Psi$  the array  $\mathbf{D}_{\gamma(s)}\mathbf{v}$  belongs to  $\mathcal{A}^r$ . On the other hand, for large  $|\gamma(s)|$  the operator  $A(\gamma(s))$  gets closer to the identity (at least on low scales) and the norm becomes closer to the  $L_2(\Omega)$ -norm so that Assumption 2 becomes less demanding. Nevertheless, the validity of (4.23) as well as of Assumption 2 is crucial for the above reasoning.

Finally, let us quickly address the estimation of  $N_L$ . A qualitative estimate on the  $L_\infty$ -norm of the integrand  $F$  is at best of the order  $e^{t\lambda_K}$ . Since the required quadrature accuracy in **Apply** is of the order  $\eta = \delta/\sigma_K$  we have to ensure, in view of (4.27), that  $\delta/\sigma_K \sim 1/(\sigma_K e^{2qN})$ . Although we do not know  $q$  we see that  $N \sim |\log \delta|$ . Thus, by (5.15), the overall work count can at best be expected to be of the order  $|\log \delta| \delta^{-1/s}$  which would almost correspond to the sparseness of  $x^\dagger = u(0)$ .

**6. Numerical Experiments.** For the numerical experiments, we choose the operator  $A = -\Delta$  with homogeneous boundary conditions on the unit interval  $\Omega = (0, 1)$ . The eigenvalues and corresponding eigenvectors of this operator are given by

$$\lambda_k = \pi^2 k^2, \quad v_k = \sqrt{2} \sin(k\pi x), \quad k = 1, 2, \dots$$

We will exploit this orthonormal basis of  $L_2(\Omega)$  to obtain a reference solution in the following experiment. Furthermore, we use the wavelet basis constructed in [6] of order 3 on the primal and dual side for the spatial discretization.. In all computations, a highest level of  $J = 15$  is fixed.

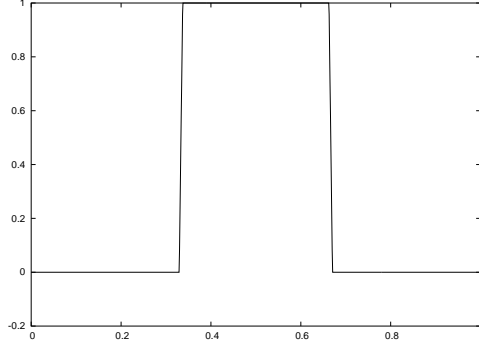


FIGURE 6.1. *Initial value*

**6.1. Application of Projections.** First, the projection of a vector  $u_0 \in L_2(\Omega)$  into the joint eigenspaces of  $A$  and  $e^{-tA}$  is tested. The main concern is to justify Assumption 1 which the adaptive projection algorithm is based upon.

For the value  $u_0$  we choose the characteristic function of  $[1/3, 2/3]$ , see figure 6.1. Its expansion into the eigenvector basis of  $A$  can easily be calculated and the Fourier coefficients with respect to this basis decay sufficiently slowly to pose a meaningful test.

To apply the projection  $\mathbf{PE}(0)$  and the projected semigroup  $\mathbf{PE}(t)$  we choose the path of integration as an ellipse

$$\gamma(s) = c + a \cos(s) + ib \sin(s), \quad s \in [0, 2\pi),$$

enclosing the eigenvalues  $\lambda_1, \lambda_2, \dots, \lambda_K$  for some fixed  $K > 0$ . The most satisfactory results are obtained by the choice

$$c = (\lambda_1 + \lambda_K)/2, \quad a = (\lambda_K - \lambda_1)/2 + 8K, \quad b = a/K.$$

To justify Assumption 1 we compare the true error

$$\text{err}(N) := \|\langle \tilde{\Psi}, Q_N(F) - e^{-tA} P_\Gamma u_0 \rangle\|_{\ell_2(\mathcal{J})} \sim \|Q_N(F)u_0 - e^{-tA} P_\Gamma u_0\|_{L_2(\Omega)}$$

with the error estimator

$$[\text{err}(N)] := \|\langle \tilde{\Psi}, Q_N(F) - Q_{2N}(F) \rangle\|_{\ell_2(\mathcal{J})} \sim \|Q_N(F)u_0 - Q_{2N}(F)u_0\|_{L_2(\Omega)}$$

for the three time steps  $t = -0.01, 0$ , and  $0.01$  and  $K = 2, 4, 6, 8$ . The arising elliptic equations are solved up to machine accuracy. This latter accuracy is chosen only in order to validate Assumption 1 and should not be confused with the adapted tolerances in **Solve** as part of the numerical solution process.

In Figures 6.2, 6.3, and 6.4 we have plotted the true error and the error estimator as functions of  $N$ . Since the true error and the error estimator are too close in the graphical displays the ratio between true error and error estimator is additionally depicted as dotted line.

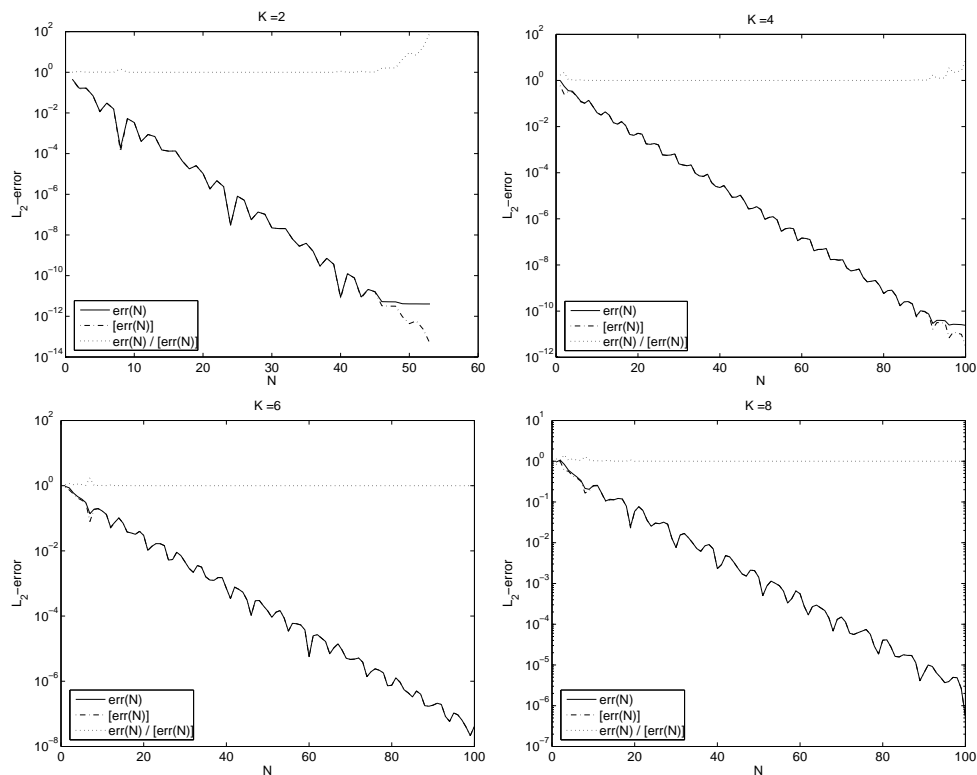


FIGURE 6.2. True error compared to error estimator for projection  $P_K u_0$

We observe an exponential convergence with respect to  $N$  as predicted by Theorem 4.1. The oscillating behavior of the error seems to be caused by the symmetry of the integrand with respect to the real axis which was not taken into account by the analysis. It should be noted that the error estimator shows the same oscillatory behavior.

The speed of convergence becomes slower for increasing values of  $K$ . This indicates that  $q > 0$ , the width of the strip  $\mathcal{D}_q$  to which  $\gamma$  extends analytically, decreases for increasing  $K$ . As for large  $K$ , the parameterization  $\gamma$  introduces a strong distortion of the complex plane, this effect is not surprising. It could be avoided by splitting  $\Gamma$  into several curves each enclosing one or a few neighboring eigenvalues.

When solving the backward problem, i.e.  $t = -0.01$ , for  $K = 8$  the absolute error is substantially larger than for the other test cases. This effect is caused by the ill-posedness of the backward problem. For  $t = -0.01$  the projected semigroup  $e^{-tA} P_\Gamma$  has the highest eigenvalue  $e^{-t\lambda_8} = 553.6 \dots$ . Thus, some of the Fourier modes of  $u_0$  are amplified substantially which results in a large norm of  $e^{-tA} P_\Gamma u_0$  and an increased absolute error.

Concerning the quality of the error estimator we obtain a ratio of almost one between the true error and the estimated one. This close relation only breaks down for large  $N$  when the quadrature error drops below  $10^{-8}$  which corresponds to the discretization error in  $H_0^1(\Omega)$  when the wavelet basis is truncated at  $J = 15$ . Thus, the breakdown of the error estimator for large values of  $N$  seems to be caused by discretization errors. Thus, Assumption 1 is justified in our test case.

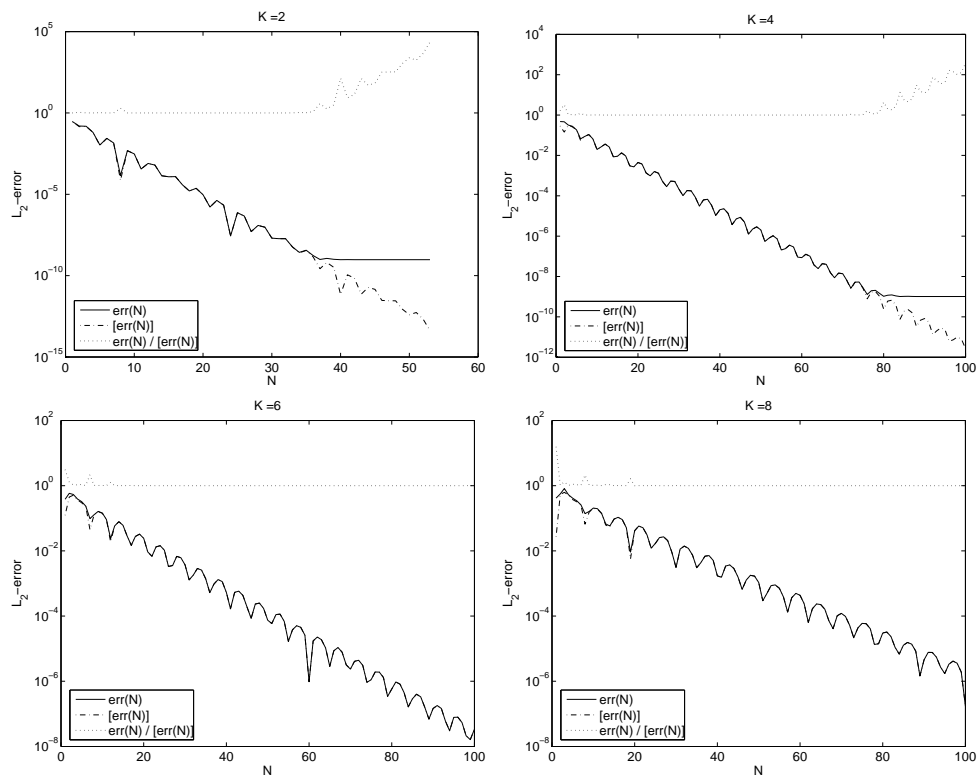


FIGURE 6.3. True error compared to error estimator for projected semigroup  $e^{-0.01A}P_K u_0$

As the error estimator is almost equal to the true error already for small  $N$ , we choose the constants from the *adaptive algorithm* to be  $N_0 = 5$  and  $\varrho = \frac{1}{3}$  and test its reliability. In this experiment we observe that the actual error stays well below the target accuracy  $\eta > 0$ . Moreover, the actual error is roughly proportional to  $\eta$  which indicates that the analysis of Lemma 4.2 is not too pessimistic. We do not provide a graphical display of this results because there is no further insight to be gained from the plot.

**6.2. Comparison of the four schemes.** We strive to recover  $x^\dagger = u_0$  from approximations  $y^\delta$  to  $y = u(t) = e^{-tA}u_0$ ,  $t = 0.01$ , where the initial value is given by  $u_0(x) = \exp(\sin(2\pi x)) - 1$ ,  $x \in (0, 1)$ . The perturbation  $y^\delta - y$  is created by adding white noise to the wavelet coefficients (normalized in  $L_2(0, 1)$ ) such that error in the discrete  $L_2(0, 1)$  norm becomes exactly  $\delta$ .

The four algorithms from Section 5 will be compared by measuring the difference of the regularized solution and the true one in the discrete  $L_2(\Omega)$ -norm, i.e.  $\|x_\alpha^\delta - x^\dagger\|_{L_2(\Omega)}$  when the perturbation  $\delta > 0$  tends to zero. The regularization parameter  $\alpha$  will be chosen according to the discrepancy principle.

The results are reported in Figure 6.5. First, we observe that the conventional Tikhonov scheme and the modified one yield the same errors. This is somewhat disappointing as the modified Tikhonov scheme seems to be superior to the usual one by its construction. Nevertheless, the experiments indicate that the additional effort for applying the projection does not pay off.

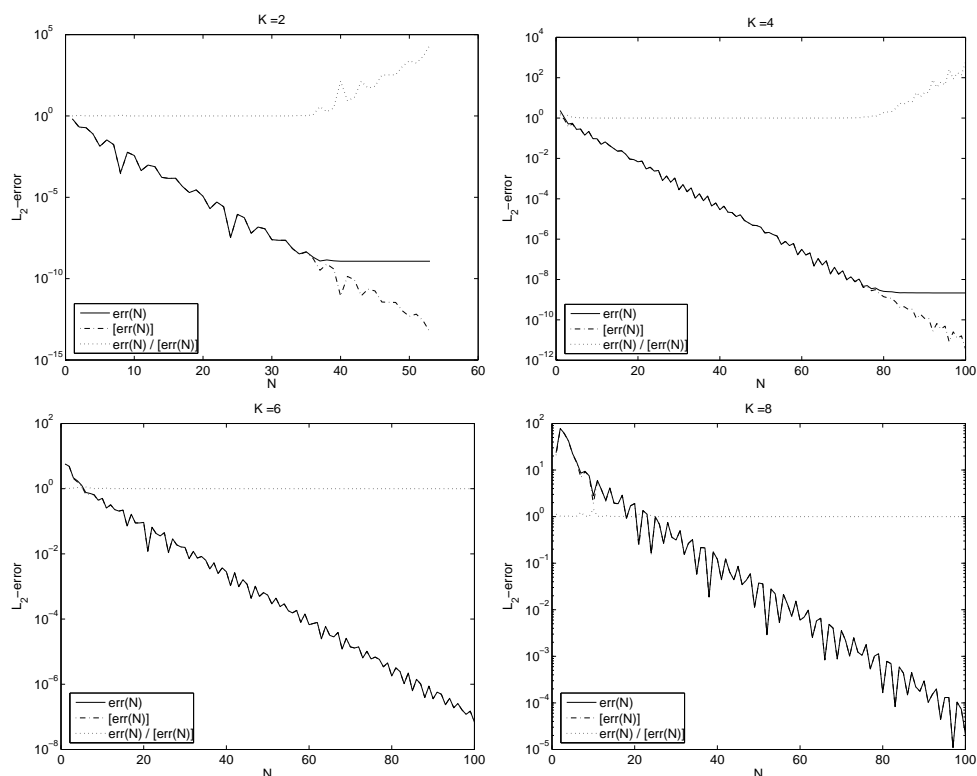


FIGURE 6.4. True error compared to error estimator for projected semigroup  $e^{0.01A} P_K u_0$

Second, the regularization in the discrete setting with  $s = 0$  produce an error close to the error of the Tikhonov regularization, but the methods with  $s = -1/2$  and  $s = -1$  yield more accurate approximations to  $x^\dagger$  for large data errors  $\delta$ . This effect was by no means clear in advance, as these methods regularize in norms different from  $\|\cdot\|_{L_2(0,1)}$ , in which the error was measured.

Third, we notice that the projection method yields errors  $\|x_\alpha^\delta - x\|_{L_2(0,1)}$  which are much smaller than those of the other three methods. Since this method requires also less computational effort than the other methods as discussed in Section 5.4 it seems to be preferable over the other three methods.

As far as can be judged from figure 6.5 none of the four methods converges with a substantially higher rate than the other ones. As the inversion of the operator exponential is a severely ill-posed problem (see [9] for a definition) there is perhaps no chance to improve on the quality of the standard methods but merely on their efficiency.

**7. Conclusions.** We have developed and implemented regularization schemes for the severely ill-posed inversion of diffusion processes. These schemes, including Tikhonov-type as well as projection methods, avoid any time stepping PDE solvers for the forward problems but rely on the error controlled approximate evaluation of certain Dunford integrals which are based on appropriate quadrature techniques and the error controlled solution of resovent systems for well-posed operators. This latter task is trivially parallelized. In particular, this allows us to realize, to our knowledge

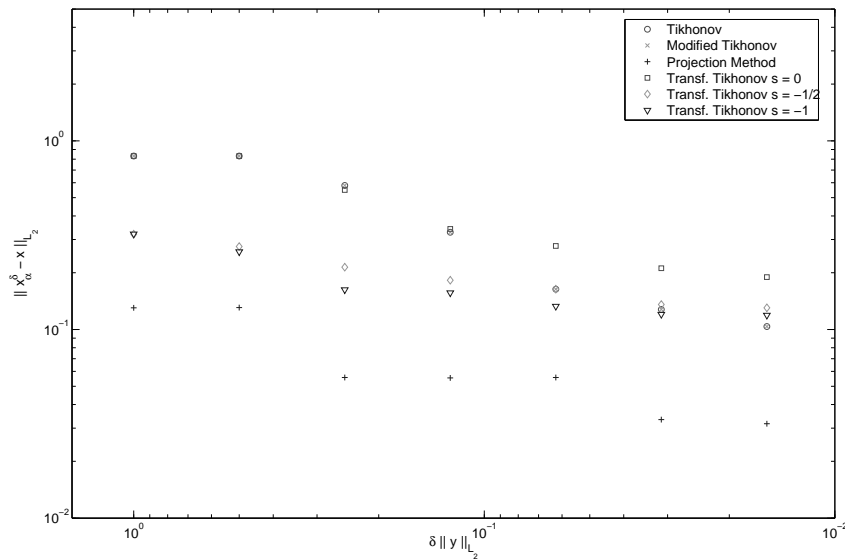


FIGURE 6.5. Comparison of Different Methods for Approximate Inversion of the Operator Exponential

for the first time in this context, SVD-projections without actually having to compute or manipulate corresponding singular basis functions. Moreover, the regularization is separated from the discretization of the diffusion operator yielding error bounds for the true infinite dimensional problem. Moreover, we present a first discussion of the complexity of the projection scheme. This together with the numerical experiments support its superiority over the Tikhonov-type schemes.

#### REFERENCES

- [1] A. Barinka, W. Dahmen, R. Schneider, Fast Computation of Adaptive Wavelet Expansions, IGPM Report, RWTH Aachen, August 2004.
- [2] A. COHEN, W. DAHMEN, AND R. DEVORE, *Adaptive wavelet methods II – Beyond the elliptic case*, *Found. Comput. Math.*, 2 (2002), pp. 203–245.
- [3] A. COHEN, M. HOFFMANN AND M. REISS, *Adaptive wavelet-galerkin methods for inverse problems*, *SIAM J. Numerical Analysis* 42 (2004), 1479–1501.
- [4] W. DAHMEN, *Wavelet and Multiscale Methods for Operator Equations*, (invited contribution) in *Acta Numerica*, Cambridge University Press, 6(1997), pp. 55–228.
- [5] W. DAHMEN, *Multiscale and Wavelet Methods for Operator Equations*, C.I.M.E. Lecture Notes in Mathematics, in *Multiscale Problems and Methods in Numerical Simulation*, Springer Lecture Notes in Mathematics, vol 1825, Springer-Verlag, Heidelberg, 2003, pp. 31–96.
- [6] W. DAHMEN, A. KUNOTH, AND K. URBAN, *Biorthogonal spline wavelets on the interval – stability and moment conditions*, *Appl. Comput. Harmon. Anal.*, 6 (1999), pp. 132–196.
- [7] W. DAHMEN AND R. SCHNEIDER, *Composite wavelet bases for operator equations*, *Math. Comput.*, 68 (1999), pp. 1533–1567.
- [8] R. DeVore, *Nonlinear approximation*, *Acta Numerica*, 7, Cambridge University Press, 1998, 51–150.
- [9] H.W. ENGL, M. HANKE, AND A. NEUBAUER, *Regularization of Inverse Problems*, Kluwer Academic Publishers, 1996.
- [10] K.-J. ENGEL AND R. NAGEL, *One-parameter Semigroups for Linear Evolution Equations*, Springer, 2000.



- [11] I. P. GAVRILYUK, W. HACKBUSCH, AND B. N. KHOROMSKIJ, *H-matrix approximation for the operator exponential with applications*, Numer. Math., 92 (2002), pp. 83–111 (2002).
- [12] T. KATO, *Perturbation Theory for Linear Operators*, Corr. printing of the 2nd ed., Springer, 1980.
- [13] R. KRESS, *Linear Integral Equations*, Springer Verlag, Berlin, 1999.
- [14] A. LUNARDY, *Analytic Semigroups and Optimal Regularity in Parabolic Problems*, Birkhäuser, 1995.
- [15] M. JÜRGENS, *A Semigroup Approach to the Numerical Solution of Parabolic Differential Equations*, PhD Dissertation, RWTH Aachen, Juli 2005.
- [16] M. JÜRGENS, *Adaptive application of the operator exponential*, submitted to J. Numer. Math., Special issue on “Breaking Complexity: Multiscale Methods for Efficient PDE Solvers”.
- [17] R. STEVENSON, *On the compressibility of operators in wavelet coordinates*, SIAM J. Math. Anal., 35 (2004), pp. 1110–1132.